TÜBİTAK

Turkish Journal of Earth Sciences

http://journals.tubitak.gov.tr/earth/

Research Article

Turkish J Earth Sci
(2016) 25: 513-537

doi:10.3906/yer-1603-7

Geochemistry and C, O, and Sr isotope composition of the Föderata Group metacarbonates (southern Veporicum, Western Carpathians, Slovakia): constraints on the nature of protolith and its depositional environment

Marek VĎAČNÝ[1,*], Peter RUŽIČKA[2], Anna VOZÁROVÁ[2]

[1]Earth Science Institute of the Slovak Academy of Sciences, Geological Division, Bratislava, Slovakia

[2]Department of Mineralogy and Petrology, Faculty of Natural Sciences, Comenius University in Bratislava, Bratislava, Slovakia

Received: 11.03.2016 • **Accepted/Published Online:** 13.07.2016 • **Final Version:** 01.12.2016

Abstract: Major, trace, and rare earth element as well as C, O, and Sr isotope geochemistry is used to provide new insights into the characteristics and depositional environment of the protolith of the Föderata Group metacarbonates in the southern Veporicum cover sequence (Western Carpathians, Slovakia). The metacarbonates are characterized by high LOI and CaO and by small contents of various insoluble components. Among the trace elements investigated, only As, Ba, Co, Cu, Hg, Nb, Ni, Pb, Rb, Sb, Sr, Th, U, Y, Zn, and Zr display concentrations beyond their detection limits. The metacarbonates are strongly depleted in Rb, Ba, Th, Nb, Hf, Zr, and Y and enriched in U and Sr relative to the UCC. Chondrite-normalized rare earth element patterns of the metacarbonates show a moderate to strong fractionation in light rare earth elements over heavy rare earth elements and distinct negative Ce and Eu anomalies. Variation plots reveal several geochemical interrelationships, among which SiO_2 – Al_2O_3 – K_2O – TiO_2 – Ba – Nb – Rb – Zr are associated with the rock's silicate fraction. The carbonate fraction comprise CaO, MgO, and Sr. The overall geochemical and C-, O-, and Sr-isotopic signatures indicate that the metacarbonates developed from sedimentary carbonate materials that were deposited in a saline, shallow-marine, low-energy environment. The negative Ce anomaly ($Ce/Ce^* = 0.15–0.93$) and the $\delta^{13}C$ (2.36‰ to –3.34‰) values indicate warmer climatic conditions during deposition. The consistency of the rock's chemical properties could be attributed to the relative stability experienced during the parent sedimentary material's deposition.

Key words: Metacarbonates, geochemistry, C-isotopes, O-isotopes, Sr-isotopes, depositional environment, southern Veporicum

1. Introduction

Marbles represent major nonmetalliferous raw materials for industries. They are a product of metamorphism of limestone that forms in a number of geochemical environments (e.g., Onimisi et al., 2013). The major constituents of marbles are calcite and subordinate dolomite, both often coexisting in a chemical equilibrium. Pure marbles (high calcium marbles), used for practical purposes, are composed primarily from calcite with a total $CaCO_3$ content ranging between 97% and 99%. On the other hand, pure dolomites contain 45.7% $MgCO_3$ and 54.3% $CaCO_3$ or 30.4% CaO and 21.8% MgO (Boynton, 1980).

Marbles studied in the present study came from the Föderata Group of the Mesozoic cover of the crystalline basement of the southern Veporic Unit (SVU) in the Western Carpathians (Slovakia). They were previously investigated with respect to P–T conditions of recrystallization by Ružička et al. (2011). These authors found that the marbles recrystallized in the low-pressure and low-temperature greenschist facies in the kyanite stability field at T_{Cal} = 354–476 °C, $T_{Ab–Or}$ = 329–453 °C, P ≈ 0.3–0.5 GPa. These P–T estimates were calculated on the basis of microprobe chemical analyses of equilibrium mineral assemblages together with analyses of bulk rock chemical composition.

In the present study, we focus on the investigation of the geochemical and C, O, and Sr isotopic features of the Föderata Group marbles to infer the nature and processes associated with the conditions of deposition of the original carbonates. The goal is to revisit issues related to the paleoenvironmental interpretations for the sedimentary basin and deepen the understanding of the geology of the cover sequence of the SVU crystalline basement.

2. Geological background

The Mesozoic Föderata Group and the Revúca Group, which comprises the Pennsylvanian Slatviná and the

* Correspondence: marek.vdacny@savba.sk

Permian Rimava Formations (Vozárová and Vozár, 1982, 1988), form the cover of the SVU crystalline basement. This cover has undergone low-grade metamorphism (e.g., Vrána, 1966; Plašienka, 1981). The presence of Pennsylvanian/Permian deposits on the one hand and the absence of Keuper facies on the other hand represent the main differences between the cover sequence of the southern Veporic and the northern Veporic Unit (Biely et al., 1996). We could only choose specific localities, because the basement of the SVU is only partly covered by the Föderata Group (Figure 1).

The Föderata Group was first defined by Rozlozsnik (1935). Maximum territorial and stratigraphic extension of this group is in the Dobšiná Brook valley. The tectonic position of the Föderata Group is in the foot wall of the Gemeric Unit, "higher" superficial nappes, and in the hanging wall of the crystalline basement of the Veporic Unit (Vojtko et al., 2000). Madarás et al. (1995) assembled the geological map of the contact zone of the Gemeric and the Veporic Units, with an emphasis on the lithostratigraphic contents of the Föderata Group.

According to lithofacies criteria and biostratigraphic data, metasedimentary rocks of the Föderata Group are of Triassic age. Specifically, dark shales forming interlayers within the black and gray crystalline limestones contain microfloral assemblages (*Leiotriletes adiantoides*, *Punctatisporites* sp., *Caythitides minor*, *Conbaculatisporites* sp., *Conbaculatisporites baculatus*, *Aratrisporites centralis*, *Anulispora foliculosa*, *Zonotriletes rotundus*) of the Ladinian-Carnian age (Biely and Planderová, 1975) and dark, sandy shales with intercalations of dark cherty limestones include conodonts (*Gondolella polygnathiformis*, *Gondolella navicula*, *Lanchodina hungarica*) of the Carnian (Cordevolian-Julian) age (Straka, 1981). A lithostratigraphically differentiated development of the Triassic metacarbonates was suggested by Plašienka (1981, 1983, 1993) due to the absence of Jurassic rocks. There are lithological differences among individual occurrences of the Föderata Group. Generally, dolomite (rauwackes), dark and light crystalline limestone, marly and siliceous cherty limestone, sandy and marly shale with lenses of dark cherty limestone, and dolomite constitute the premetamorphic Middle and Upper Triassic succession. The thickness of the Föderata Group ranges between 200 and 450 m (Biely et al., 1996).

3. Sampling and analytical methods

Twenty-nine representative unweathered rock samples weighing 1 to 2 kg were collected during fieldwork and traversing of various metacarbonate rock outcrops and quarries within the Föderata Group of the SVU. Sampling localities were in the Dobšiná Brook valley (DP), the Plačkova valley (PLD), and the surroundings of the villages of Tuhár (T) and Ružiná (R) (Figure 1). The Dobšiná Brook valley is about 4 km from the city of Dobšiná, eastern Slovakia (48°49′435″N, 20°17′689″E). The Plačkova valley is situated approximately 10 km NW of the city of Tisovec, central Slovakia (48°43′570″N, 19°50′470″E). The villages of Tuhár (48°25′340″N, 19°31′347″E) and Ružiná (48°25′566″N, 19°32′173″E) are located ca. 15 km NW of the city of Lučenec, southern Slovakia. Altogether, fourteen samples were collected in the Dobšiná Brook valley, five samples in the Plačkova valley, and eight samples in the "Tuhár Mesozoic area", whereas only a single lineated sample was collected in the vicinity of the village of Ružiná. The Ružiná sample was, however, subdivided into two samples: R-1 containing a grayish calcite-quartz band and R-2 consisting of a white, dominantly calcite band. Before transport to the laboratory, the collected samples were cleaned of evident allogenic material and/or weathered portions.

Prior to the geochemical analyses, about 1 kg of representative rock material from each sample was broken into thumbnail-sized pieces using a hardened-steel hammer. These pieces were first crushed and pulverized to particle size as fine as –60 mesh with a "jaw crusher" and then were powdered in an agate mortar to –200 mesh after being thoroughly homogenized. The powders were analyzed at Acme Analytical Laboratories Ltd. in Vancouver, Canada, for major, trace, and rare earth element (REE) contents, as well as for total carbon, sulfur, and loss-on-ignition (LOI).

LOI was assessed by igniting 400 mg of a split from each sample at 1000 °C and then the weight loss was measured. After sample ignition at >800 °C, total carbon and total sulfur concentrations were determined using a LECO carbon-sulfur analyzer. Two instruments for inductively coupled plasma optical emission spectrometry (ICP-OES) and inductively coupled plasma mass spectrometry (ICP-MS) were used for whole-rock geochemical analyses. Samples were digested by lithium metaborate/tetraborate fusion. All sample solutions were analyzed in duplicate and reproducibility was found to be within ±2%. The detection limit for all the major and minor element oxides was 0.01%, the only exceptions being Fe_2O_3 with a detection limit of 0.04%, Cr_2O_3 with 0.002%, and P_2O_5 with 0.001%. The trace element detection limits spanned a range of 0.01–1 ppm, the single exception being V with a detection limit of 8 ppm.

C and O isotope ratios in isolated CO_2 were measured in all 29 investigated metacarbonate samples at the Department of Isotope Geology of the State Geological Institute of Dionýz Štúr in Bratislava, Slovakia. The international standards V-SMOW and PDB were used to express the $\delta^{13}C$ and $\delta^{18}O$. Measurements were conducted using a Finnigan MAT 250 mass spectrometer and had

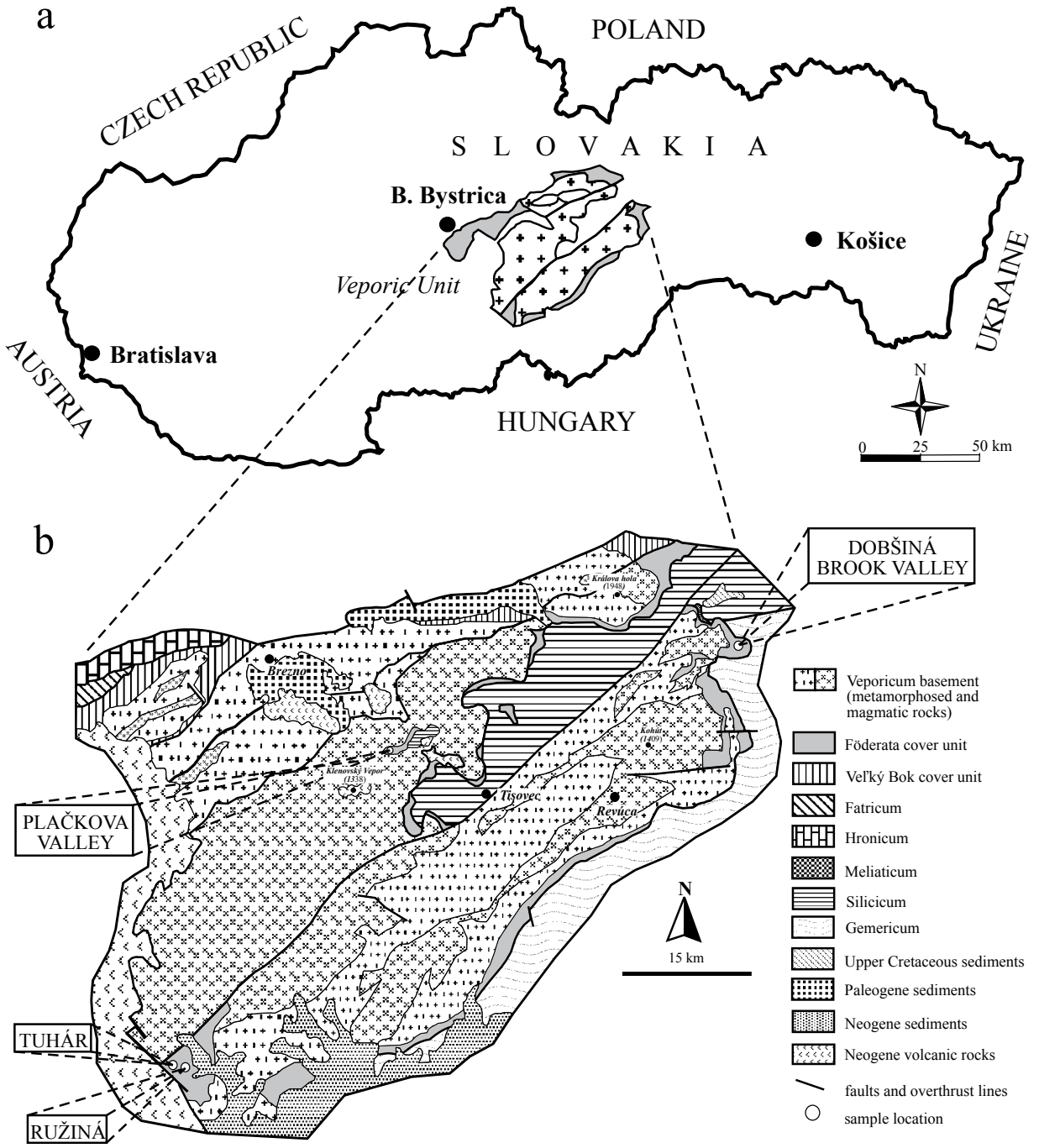

Figure 1. Tectonic sketch (after Vozár et al., 1998) and simplified geological map of the Veporicum (after Hók et al., 2001) with sample localities.

reproducibility within ±0.02‰ for both $\delta^{13}C_{PDB}$ and $\delta^{18}O_{PDB}$. Prior to analysis, all pulverized samples were ignited at 470 °C for 30 min to remove organic contaminants. CO_2 was extracted in vacuum by reaction with phosphoric acid using the method of McCrea (1950). $\delta^{18}O_{CO_2}$ values were corrected to the isotopic fractionation of oxygen between $CaCO_3$ and H_3PO_4 by the fractionation factor α of 1.01025 (Friedman and O'Neil, 1977). For carbonates soluble at higher temperature, a fractionation factor was calculated for the given temperature from the chemical composition of a carbonate (Rosenbaum and Sheppard, 1986; Carothers et al., 1988; Swart et al., 1991; Böttcher, 1996).

The $^{87}Sr/^{86}Sr$ ratios were measured at Geochron Laboratories, Billerica, MA, USA. Six metacarbonate

samples were selected for isotope determination: two samples from the Tuhár locality (T-3 and T-6), two from the Ružiná (R-1 and R-2), and two from the Dobšiná Brook valley (DP-7 and DP-10). These samples were analyzed in a thermal ionization mass spectrometer (TIMS). $^{87}Sr/^{86}Sr$ values were normalized to an $^{86}Sr/^{88}Sr$ value of 0.1194. The NIST 987 standard was routinely analyzed along with our samples and gave an average $^{87}Sr/^{86}Sr$ value of 0.710240 ± 0.000012 (2σ error). No age-corrections were considered necessary for the $^{87}Sr/^{86}Sr$ ratios, because the Rb and Sr contents determined from whole-rock powders include the effects of any minor contaminants.

4. Petrographic characteristics of the Föderata Group metacarbonates

A detailed petrographic description of the studied metacarbonates was provided by Ružička et al. (2011). Therefore, the metacarbonates are described here only briefly.

Metacarbonates from the Dobšiná Brook valley display a granoblastic texture alternating with chaotically distributed coarse-grained twinned lamellar and fine-grained calcite aggregates that grade into fine-grained mylonitic material. Dolomite porphyroblasts in these rocks form sharp-bordered rhombohedra inside polycrystalline calcite aggregates. Likewise, metacarbonates from the Plačkova valley exhibit differentiated fine- to coarse-grained calcite aggregates arranged in granoblastic textures. The equigranular calcite granoblastic microstructure of the metacarbonates from Tuhár shows slight deformation and preferred orientation, with local transitions from fine- to medium-grained matrix.

Because the Föderata Group metacarbonates contain fine-grained silicate minerals that are difficult to discern by means of optical microscope, semiquantitative X-ray diffraction analyses were carried out (Ružička, 2009). These were conducted on powdered samples under CuK_{α} graphite monochromatic radiation at 40 kV and 20 mA. The metacarbonates studied are predominantly calcitic with dolomite as subdominant, while quartz, muscovite, illite, and kaolinite constitute the accessory phases (Table 1). However, on the basis of the microprobe chemical analyses, the metamorphic/detrital mineral assemblage is sometimes slightly richer (Ružička et al., 2011). Specifically, the DP metacarbonates include calcite, dolomite, quartz, muscovite (phengite), phlogopite, K-feldspar, and albite. Further, the metamorphic mineral equilibrium assemblage of the PLD metacarbonates encompasses calcite, dolomite, quartz, muscovite (phengite), and phlogopite. Finally, the metamorphic (eventually detrital) mineral assemblage of the Tuhár rocks is represented only by calcite, dolomite, quartz, and muscovite (phengite).

5. Results and discussion

5.1. Major element oxides and relevant data

The concentrations of major element oxides and other related chemical data of the Föderata Group metacarbonates are presented in Table 2. A cursory appraisal of the data reveals that MgO, CaO, and LOI frequently constitute more than 91 wt. % of the rock composition, corroborating our previous mineralogical observations (Table 1) that the carbonate phases are the predominant phases in the metacarbonates studied (see also Ružička et al., 2011). The high LOI values are mostly due to CO_2. Also, these high LOI values certainly reflect the low silica composition of the studied rocks (Table 1). Apart from LOI, CaO represents the dominant constituent, with concentrations ranging from 37.27 to 55.55 wt. %, whereby the mean value is 51.66 wt. %. This is followed by MgO, whose concentration varies from 0.34 to 11.72 wt. %, with an average of 1.91 wt. %. We can assume that all CaO and MgO is related to calcite and dolomite. However, the true picture may be slightly different. Dolomite may not be the dominant host mineral for CaO and MgO, as indicated by the noncorrespondence of the metacarbonate sample plots with the line depicting stoichiometric dolomite on the Ca versus Mg plot (Figure 2). Further, we speculate that some MgO could be also admixed in the calcite structural lattices, which was similarly observed in the Jabal Farasan marble from central-western Saudi Arabia by Qadhi (2008). Both CaO and MgO are also possibly bound in the structure of the small and probably insignificant silicate phases that are represented by quartz, muscovite, phlogopite, K-feldspar, albite, illite, and kaolinite, all constituting parts of the modal mineralogy of the Föderata Group metacarbonates (Table 1 and Ružička et al., 2011).

Insoluble residues, notably, SiO_2 (0.28–29.92 wt. %) and Al_2O_3 (0.01–2.99 wt. %), have low abundances. Generally, silica in carbonate rocks comes from both silicate minerals and chert nodules, resulting from the influx of near-shore materials into the depositional basin of limestones prior to metamorphism (Brownlow, 1996). Clearly the silica content in the metacarbonate samples varies widely (Table 2). We assume that the relatively high content of silica in some samples can be attributed to a shallower depth of deposition of the premetamorphic limestone.

Except for sample PLD-1, Fe_2O_3 is less than 0.91 wt. %, while TiO_2, Cr_2O_3, MnO, Na_2O, K_2O, and P_2O_5 concentrations are negligible (Table 2). The alkali elements, Na and K, are indicative of salinity levels (Onimisi et al., 2013) and, as shown by Land and Hoops (1973), they are very useful in interpreting depositional and lithification conditions of carbonates. The concentration of the total alkalis ($Na_2O + K_2O$) in the Föderata Group metacarbonates is very low, in each case less than 1 wt. %. According to Clarke (1924), Na and K concentration in marbles tends

Table 1. Semiquantitative X-ray diffraction data of the Föderata Group metacarbonates.

Sample	Calcite	Dolomite	Quartz	Muscovite	Illite	Kaolinite
T-1	D	SD	n.d.	n.d.	n.d.	n.d.
T-2	D	SD	n.d.	n.d.	AC	n.d.
T-3	D	SD	n.d.	n.d.	AC	n.d.
T-4	D	AC	n.d.	n.d.	AC	n.d.
T-5	D	SD	n.d.	n.d.	n.d.	n.d.
T-6	D	SD	n.d.	n.d.	n.d.	n.d.
T-7	D	SD	n.d.	n.d.	n.d.	n.d.
T-8	D	n.d.	n.d.	n.d.	n.d.	n.d.
R-1	D	AC	SD	TR	n.d.	n.d.
R-2	D	AC	n.d.	n.d.	n.d.	n.d.
PLD-1	D	TR	AC	AC	n.d.	AC
PLD-2	D	AC	TR	AC	n.d.	TR
PLD-3	D	AC	AC	AC	n.d.	n.d.
PLD-4	D	TR	AC	AC	n.d.	n.d.
PLD-5	D	AC	AC	AC	n.d.	TR
DP-1	D	SD	AC	n.d.	n.d.	n.d.
DP-2	D	SD	TR	n.d.	AC	n.d.
DP-3	D	n.d.	AC	AC	n.d.	n.d.
DP-4	D	SD	AC	AC	n.d.	n.d.
DP-5	D	n.d.	n.d.	AC	n.d.	n.d.
DP-6	D	SD	n.d.	TR	n.d.	n.d.
DP-7	D	AC	AC	TR	n.d.	n.d.
DP-8	D	n.d.	n.d.	n.d.	n.d.	n.d.
DP-9	D	AC	TR	n.d.	n.d.	n.d.
DP-10	D	TR	AC	n.d.	n.d.	n.d.
DP-11	D	D	n.d.	AC	n.d.	n.d.
DP-12	D	SD	TR	AC	n.d.	n.d.
DP-13	D	AC	n.d.	AC	n.d.	n.d.
DP-14	D	AC	n.d.	AC	n.d.	n.d.

D = Dominant (>50%); SD = subdominant (20%–50%); AC = accessory (5%–20%); TR = trace («5%); n.d. = not detected.

to decrease with increasing salinity. The low values of total alkali content in the Föderata Group metacarbonates indicate that the depositional environment of the original carbonates might have been a shallow, highly saline environment. Furthermore, the relatively low abundance of Fe, Mn, and P in the samples studied probably reflects low detrital and organic inputs (Tucker, 1983).

As expected for carbonate-bearing rocks, the total carbon values are high, i.e. spanning a range of 8.49–12.80 wt. % with an average of 11.76 wt. % (Table 2). On the other hand, the total sulfur concentration is generally below the 0.02 wt. % detection limit.

5.2. Trace element composition

Trace element data of the studied metacarbonates are summarized in Table 3. Only As, Ba, Co, Cu, Hg, Nb, Ni, Pb, Rb, Sb, Sr, Th, U, Y, Zn, and Zr were above their detection limits. The rock's trace element concentrations are not as low as expected and Sr and Ba values are highly variable (Table 3). This possibly suggests a complex distribution of the elements (Georgieva et al., 2009). As concerns concentrations of large ion lithophile elements (LILEs), Ba (22.2 ppm on average), Sr (669 ppm on average), and probably Rb (5.9 ppm on average) are considered moderate. Given the fact that Sr content of recent carbonates is

Table 2. Concentrations of the major element oxides and related chemical data of metacarbonate rocks of the Föderata Group.

	T-1	T-2	T-3	T-4	T-5	T-6	T-7	T-8	R-1	R-2	PLD-1	PLD-2	PLD-3	PLD-4	PLD-5
Major element oxide, total carbon, and LOI compositions (%)															
SiO_2	0.68	0.71	0.55	0.45	0.40	0.73	0.28	0.91	29.92	1.07	15.09	13.31	4.44	6.97	5.02
TiO_2	<0.01	<0.01	0.01	<0.01	<0.01	0.01	<0.01	<0.01	<0.01	0.01	0.12	0.13	0.06	0.04	0.03
Al_2O_3	0.21	0.24	0.29	0.13	0.19	0.30	0.14	0.21	0.30	0.29	2.89	2.99	1.42	0.79	0.82
Cr_2O_3	<0.002	<0.002	<0.002	<0.002	<0.002	<0.002	<0.002	<0.002	<0.002	<0.002	0.007	0.006	<0.002	<0.002	<0.002
Fe_2O_3	0.23	0.15	0.21	0.14	0.39	0.25	0.16	0.21	0.25	0.16	1.22	0.91	0.46	0.26	0.29
MnO	0.02	0.01	0.02	0.01	0.02	0.02	0.02	0.02	0.02	0.02	0.05	0.06	<0.01	0.02	0.01
MgO	1.57	1.41	1.21	1.16	1.94	1.44	1.44	0.70	1.38	1.47	0.96	0.67	2.75	0.91	2.29
CaO	54.39	54.98	54.67	55.50	54.02	54.89	55.46	55.28	37.27	53.32	43.76	45.35	48.49	50.11	50.36
Na_2O	<0.01	<0.01	<0.01	<0.01	<0.01	<0.01	<0.01	<0.01	<0.01	<0.01	0.04	0.16	<0.01	<0.01	<0.01
K_2O	0.08	0.08	0.09	0.05	0.04	0.11	0.03	0.07	0.10	0.08	0.78	0.84	0.56	0.31	0.15
P_2O_5	0.030	0.021	0.031	0.042	0.032	0.062	0.027	0.034	0.049	0.041	0.070	0.060	0.060	0.030	0.020
LOI	42.2	42.9	43.4	42.8	43.2	42.5	42.4	42.2	30.8	42.9	34.9	35.5	41.6	40.5	40.9
Total	99.43	100.52	100.49	100.30	100.25	100.32	99.98	99.66	100.11	99.37	99.89	99.99	99.86	99.95	99.90
Total carbon	12.28	12.19	12.17	12.42	11.88	11.92	12.40	11.86	8.49	12.24	9.74	9.82	11.44	11.07	11.39
Elemental abundance (%)															
Si	0.32	0.33	0.26	0.21	0.19	0.34	0.13	0.42	13.97	0.50	7.05	6.22	2.07	3.25	2.34
Ti	0.00	0.00	0.00	0.00	0.00	0.00	0.00	0.00	0.00	0.00	0.07	0.08	0.04	0.02	0.02
Al	0.06	0.06	0.08	0.03	0.05	0.08	0.04	0.06	0.08	0.08	0.77	0.79	0.38	0.21	0.22
Cr	0.00	0.00	0.00	0.00	0.00	0.00	0.00	0.00	0.00	0.00	0.002	0.002	0.000	0.000	0.000
Fe	0.18	0.12	0.16	0.11	0.30	0.19	0.12	0.16	0.19	0.12	0.95	0.71	0.36	0.20	0.23
Mn	0.02	0.01	0.02	0.01	0.02	0.02	0.02	0.02	0.02	0.02	0.04	0.05	0.00	0.02	0.01
Mg	0.95	0.85	0.73	0.70	1.17	0.87	0.87	0.42	0.83	0.89	0.58	0.40	1.66	0.55	1.38
Ca	38.89	39.31	39.09	39.68	38.62	39.25	39.65	39.53	26.65	38.12	31.29	32.43	34.67	35.83	36.01
Na	0.00	0.00	0.00	0.00	0.00	0.00	0.00	0.00	0.00	0.00	0.01	0.06	0.00	0.00	0.00
K	0.03	0.03	0.04	0.02	0.02	0.05	0.01	0.03	0.04	0.03	0.32	0.35	0.23	0.13	0.06
P	0.007	0.005	0.007	0.009	0.007	0.014	0.006	0.007	0.011	0.009	0.015	0.013	0.013	0.007	0.004

Table 2. (Continued).

	DP-1	DP-2	DP-3	DP-4	DP-5	DP-6	DP-7	DP-8	DP-9	DP-10	DP-11	DP-12	DP-13	DP-14
Major element oxide, total carbon, and LOI compositions (%)														
SiO_2	1.34	2.22	3.50	4.41	2.20	1.33	1.98	0.47	1.09	2.52	0.63	1.00	0.90	1.26
TiO_2	<0.01	0.03	0.05	0.03	0.02	0.01	0.02	<0.01	<0.01	0.01	<0.01	0.01	<0.01	<0.01
Al_2O_3	0.23	0.70	1.23	0.84	0.75	0.27	0.42	0.09	0.21	0.42	0.12	0.33	0.25	0.01
Cr_2O_3	<0.002	<0.002	<0.002	<0.002	<0.002	<0.002	<0.002	<0.002	<0.002	<0.002	<0.002	<0.002	<0.002	<0.002
Fe_2O_3	0.22	0.25	0.39	0.38	0.10	0.12	0.17	0.06	0.06	0.15	<0.04	0.08	0.06	<0.04
MnO	<0.01	<0.01	<0.01	0.01	<0.01	<0.01	<0.01	<0.01	<0.01	<0.01	<0.01	<0.01	<0.01	<0.01
MgO	1.97	3.22	1.06	3.19	0.49	3.96	0.78	0.34	1.15	0.59	11.72	3.28	2.02	0.41
CaO	53.98	52.07	51.38	47.96	53.10	50.44	53.42	55.31	54.47	53.38	42.99	52.31	53.88	55.55

Table 2. (Continued).

Na_2O	0.02	0.01	<0.01	0.02	<0.01	<0.01	<0.01	<0.01	<0.01	0.03	<0.01	<0.01	<0.01	<0.01
K_2O	0.14	0.30	0.61	0.27	0.25	0.10	0.23	0.06	0.12	0.16	0.05	0.11	0.10	<0.01
P_2O_5	0.029	0.027	0.070	0.025	0.001	0.021	0.006	<0.001	0.012	0.024	<0.010	0.020	<0.010	<0.010
LOI	41.8	40.3	40.9	42.0	41.3	42.2	41.8	42.4	42.3	41.9	44.2	42.6	42.6	42.5
Total	99.75	99.14	99.21	99.14	98.23	98.47	98.85	98.76	99.44	99.20	99.79	99.76	99.85	99.82
Total carbon	12.57	12.28	12.00	11.86	12.80	12.45	11.74	11.78	12.23	12.34	12.40	11.53	11.90	11.89
Elemental abundance (%)														
Si	0.63	1.04	1.63	2.06	1.03	0.62	0.92	0.22	0.51	1.18	0.29	0.47	0.42	0.59
Ti	0.00	0.02	0.03	0.02	0.01	0.01	0.01	0.00	0.00	0.01	0.00	0.01	0.00	0.00
Al	0.06	0.19	0.33	0.22	0.20	0.07	0.11	0.02	0.06	0.11	0.03	0.09	0.07	0.00
Cr	0.00	0.00	0.00	0.00	0.00	0.00	0.00	0.00	0.00	0.00	0.00	0.00	0.00	0.00
Fe	0.17	0.19	0.30	0.30	0.08	0.09	0.13	0.05	0.05	0.12	0.00	0.06	0.05	0.00
Mn	0.00	0.00	0.00	0.00	0.00	0.00	0.00	0.00	0.00	0.00	0.00	0.00	0.00	0.00
Mg	1.19	1.94	0.64	1.92	0.30	2.39	0.47	0.21	0.69	0.36	7.07	1.98	1.22	0.25
Ca	38.60	37.23	36.74	34.29	37.97	36.06	38.20	39.55	38.95	38.17	30.74	37.40	38.52	39.72
Na	0.01	0.00	0.00	0.01	0.00	0.00	0.00	0.00	0.00	0.01	0.00	0.00	0.00	0.00
K	0.06	0.12	0.25	0.11	0.10	0.04	0.10	0.02	0.05	0.07	0.02	0.05	0.04	0.00
P	0.006	0.006	0.015	0.005	0.000	0.005	0.001	0.000	0.003	0.005	0.000	0.004	0.000	0.000

expected to range from 30 to 200 ppm (Shearman and Shirmohammadi, 1969), the Sr concentration of the Föderata Group metacarbonates appears to be appropriate. Among the high-charged cations, Zr has concentrations ranging from 0.1 to 21.3 ppm (5.3 ppm on average), Nb from 0.1 to 2.5 ppm (0.7 ppm on average), and U from 0.1 to 4.3 ppm. Y concentration varies from 0.4 to 15.1 ppm. Ni (5.3 ppm on average), As (4.8 ppm on average), Zn (3.6 ppm on average), Pb (2.6 ppm on average), and Co (1.1 ppm on average) display moderate concentrations, while those of Sb (0.8 ppm on average), Th (0.8 ppm on average), Cu (0.7 ppm on average), and Hg (0.04 ppm on average) appear low. Figure 3 illustrates the trace element composition of the metacarbonate rocks studied normalized to the average upper continental crust (UCC) of Taylor and McLennan (1981). As can be noted, the metacarbonates are strongly depleted in Rb, Ba, Th, Nb, Hf, Zr, and Y and enriched in U and Sr relative to the UCC.

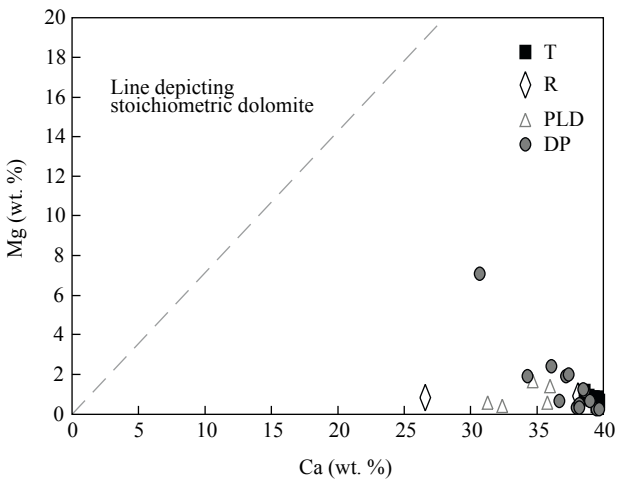

Figure 2. Comparison of the calcium and magnesium contents of the Föderata Group metacarbonates with the ratio characteristics of stoichiometric dolomite (modified from Johnson et al., 2010).

A study of trace elements in metamorphic rocks provides a unique way to infer the nature of the premetamorphic material, because some sedimentary rocks exhibit unique assemblages of these elements. Immobile trace elements such as the high field strength elements (HFSEs) are an important tool for determination of pelitic rock provenance (Taylor and McLennan, 1985), since their concentrations often reflect those of their source rock. The majority of rarer elements are more abundant in shale than in sandstones and limestone (Krauskopf and Bird, 1995). Strontium and manganese are major exceptions, as they are significantly enriched in carbonate sediments. The enrichment of strontium in limestone is interpreted such that Sr^{2+} substitutes readily for the very similar ion Ca^{2+}. A similar ionic size is also probably the reason for the smaller but appreciable concentration of manganese in carbonates. A comparison of Ni, Zn, Sr, and Mn content in the metacarbonate samples studied with

Table 3. Trace element composition (ppm) and relevant ratios of metacarbonate rocks of the Föderata Group.

	T-1	T-2	T-3	T-4	T-5	T-6	T-7	T-8	R-1	R-2	PLD-1	PLD-2	PLD-3	PLD-4	PLD-5
As	0.5	<0.5	0.8	<0.5	1.4	<0.5	0.7	<0.5	<0.5	<0.5	22.3	29.7	9.0	7.3	14.2
Ba	14	2	5	5	11	10	8	6	4	5	164	167	37	23	18
Cd	0.2	0.3	0.3	0.3	0.2	0.3	0.3	0.2	0.1	0.1	<0.1	<0.1	<0.1	0.2	<0.1
Co	0.6	0.9	1.3	0.5	1.5	1.0	0.6	1.1	1.1	2.1	5.2	4.2	0.8	1.0	0.3
Cs	<0.1	<0.1	<0.1	<0.1	<0.1	<0.1	<0.1	<0.1	0.1	<0.1	0.7	0.8	0.9	0.3	0.8
Cu	1.3	0.4	0.2	0.2	0.5	0.3	0.4	0.8	<0.1	1.1	0.1	0.7	1.0	1.2	<0.1
Ga	<0.5	<0.5	<0.5	0.6	<0.5	<0.5	<0.5	0.5	1.2	<0.5	3.5	3.5	1.8	0.9	1.2
Hf	<0.1	<0.1	<0.1	<0.1	<0.1	<0.1	<0.1	<0.1	<0.1	0.1	0.6	0.6	0.5	0.5	0.2
Hg	0.03	0.03	<0.01	0.02	0.02	<0.01	<0.01	0.02	<0.01	0.01	0.09	0.03	<0.01	0.01	0.02
Mo	<0.1	<0.1	<0.1	<0.1	<0.1	<0.1	<0.1	<0.1	<0.1	<0.1	0.2	0.3	0.9	0.2	3.3
Nb	0.3	0.6	0.4	0.3	0.1	0.7	<0.1	0.3	0.3	0.3	2.3	2.5	1.4	1.0	0.8
Ni	3.3	3.4	5.1	3.1	5.7	5.8	5.3	3.5	4.0	5.5	23.0	24.3	3.9	1.7	1.9
Pb	3.5	1.4	1.8	1.4	1.9	1.1	2.0	1.4	1.1	1.8	0.6	0.7	2.4	2.6	4.7
Rb	2.5	2.2	2.9	1.1	1.5	2.7	0.8	2.5	3.2	2.8	27.0	26.7	15.2	7.5	5.2
Sb	0.2	<0.1	<0.1	<0.1	0.3	<0.1	<0.1	0.3	<0.1	0.3	0.2	1.3	0.5	0.3	0.5
Sc	1	<1	1	<1	1	1	<1	2	1	1	3	4	1	1	<1
Se	<0.5	<0.5	<0.5	<0.5	<0.5	<0.5	<0.5	<0.5	<0.5	<0.5	0.7	<0.5	<0.5	<0.5	<0.5
Sr	184.5	152.5	221.7	169.8	193.9	199.0	184.6	197.2	109.4	132.6	365.8	294.8	426.4	198.0	260.0
Ta	<0.1	<0.1	<0.1	<0.1	<0.1	<0.1	<0.1	<0.1	<0.1	<0.1	0.1	0.2	<0.1	0.1	<0.1
Th	0.5	0.4	0.4	0.7	0.9	0.5	0.6	0.8	0.6	0.8	1.7	2.2	1.5	3.4	0.8
Tl	<0.1	<0.1	<0.1	<0.1	<0.1	<0.1	<0.1	<0.1	<0.1	<0.1	<0.1	<0.1	<0.1	<0.1	<0.1
U	0.1	0.1	0.1	<0.1	0.4	0.1	<0.1	<0.1	0.4	1.2	1.5	1.6	2.8	0.8	4.3
V	<8	<8	<8	<8	<8	<8	<8	<8	15	14	42	41	24	13	24
W	<0.5	<0.5	<0.5	<0.5	<0.5	<0.5	<0.5	<0.5	<0.5	<0.5	1.2	1.2	<0.5	<0.5	<0.5
Y	9.8	6.5	6.6	9.1	10.3	9.2	8.6	11.9	11.6	14.2	13.1	12.4	11.3	15.1	2.0
Zn	4	3	3	3	6	4	3	3	4	8	1	1	5	8	2
Zr	1.7	3.3	3.6	1.2	1.7	2.7	0.9	2.4	2.3	3.0	21.3	21.1	15.3	14.6	7.7
Mn/Sr	0.84	0.50	0.70	0.45	0.80	0.78	0.84	0.79	1.42	1.17	1.06	1.57	0.18	0.78	0.30
Mg/Ca	0.02	0.02	0.02	0.02	0.03	0.02	0.02	0.01	0.03	0.02	0.02	0.01	0.05	0.02	0.04

Table 3. (Continued).

	DP-1	DP-2	DP-3	DP-4	DP-5	DP-6	DP-7	DP-8	DP-9	DP-10	DP-11	DP-12	DP-13	DP-14
As	1.3	2.8	4.8	1.5	0.6	2.3	0.7	<0.5	0.9	2.5	6.7	8.2	9.2	8.2
Ba	5	17	26	24	15	19	8	<1	4	22	6	6	10	2
Cd	<0.1	<0.1	<0.1	0.2	<0.1	<0.1	<0.1	<0.1	<0.1	<0.1	<0.1	<0.1	<0.1	2.5
Co	<0.2	0.4	1.9	1.5	1.2	0.5	0.7	0.4	0.7	0.8	<0.2	<0.2	<0.2	<0.2
Cs	<0.1	0.2	1.1	0.7	<0.1	<0.1	0.2	<0.1	<0.1	0.2	<0.1	<0.1	<0.1	<0.1
Cu	0.9	0.8	1.9	2.2	0.5	0.4	0.6	0.3	0.5	1.5	<0.1	<0.1	1.0	<0.1
Ga	<0.5	1.1	1.3	1.3	0.9	<0.5	0.5	<0.5	<0.5	0.7	<0.5	<0.5	<0.5	<0.5
Hf	<0.1	<0.1	0.4	0.2	0.2	<0.1	0.2	<0.1	<0.1	<0.1	<0.1	<0.1	<0.1	<0.1

Table 3. (Continued).

Hg	<0.01	<0.01	<0.01	0.07	<0.01	<0.01	0.12	0.08	0.18	0.04	0.01	0.01	0.02	0.21
Mo	<0.1	<0.1	<0.1	0.2	<0.1	<0.1	<0.1	<0.1	<0.1	0.2	0.1	0.1	0.2	0.1
Nb	0.4	0.5	1.6	1.2	0.8	0.3	0.7	0.3	0.2	0.4	1.4	0.2	0.2	<0.1
Ni	3.1	5.1	4.6	4.6	4.2	3.3	3.5	4.4	4.5	5.5	1.9	3.3	2.0	3.1
Pb	0.6	1.1	1.7	7.6	0.5	5.5	1.1	0.4	1.0	2.8	0.5	0.4	2.0	20.8
Rb	2.7	8.5	19.0	10.5	5.7	3.0	4.8	1.2	2.4	3.8	1.1	2.5	2.1	0.1
Sb	0.6	1.6	4.1	4.6	1.1	1.4	1.1	0.3	1.3	0.6	0.3	0.6	0.9	1.5
Sc	<1	<1	<1	1	<1	<1	<1	<1	<1	<1	<1	<1	<1	<1
Se	<0.5	<0.5	<0.5	<0.5	<0.5	1.0	0.5	<0.5	<0.5	<0.5	<0.5	<0.5	<0.5	<0.5
Sr	516.1	551.5	351.4	403.5	1779.0	471.2	2683.0	1961.0	970.1	2607.0	258.1	1060.0	1334.0	1164.0
Ta	<0.1	<0.1	0.1	<0.1	<0.1	<0.1	<0.1	<0.1	<0.1	<0.1	<0.1	<0.1	<0.1	<0.1
Th	0.3	0.6	1.1	1.4	0.8	0.3	0.5	<0.2	0.2	<0.2	0.2	<0.2	<0.2	<0.2
Tl	<0.1	<0.1	0.1	<0.1	<0.1	<0.1	<0.1	<0.1	<0.1	<0.1	<0.1	<0.1	<0.1	<0.1
U	1.0	1.1	0.9	0.9	0.9	0.6	1.1	0.9	1.0	0.9	0.7	0.7	0.8	1.0
V	<8	<8	10	<8	<8	<8	<8	<8	<8	19	13	9	14	<8
W	<0.5	<0.5	6.1	3.7	1.8	<0.5	<0.5	<0.5	<0.5	<0.5	<0.5	<0.5	<0.5	<0.5
Y	5.3	3.7	4.9	6.6	1.1	7.5	7.0	0.4	0.7	9.0	0.7	0.7	1.3	0.4
Zn	<1	2	4	8	1	4	4	<1	2	3	<1	<1	<1	14
Zr	3.8	4.5	12.7	7.5	5.3	3.1	5.8	1.0	1.6	2.7	0.9	1.6	1.6	0.1
Mn/Sr	0.15	0.14	0.22	0.19	0.04	0.16	0.03	0.04	0.08	0.03	0.30	0.07	0.06	0.07
Mg/Ca	0.03	0.05	0.02	0.06	0.01	0.07	0.01	0.01	0.02	0.01	0.23	0.05	0.03	0.01

that in known sedimentary carbonates (the protolith of metacarbonates) is provided in Table 4. Concentrations of the aforementioned elements in the metacarbonates studied are quite similar to those in sedimentary carbonates. Therefore, concentrations of Ni, Zn, Sr, and Mn in the metacarbonates investigated very likely reflect those of their source rocks. The lower content of Sr and Mn in some samples relative to that in sedimentary carbonates may be attributed to the substitution of Sr and Mn by Ca, which took place during the recrystallization of the mineral grains at higher temperatures during the metamorphism.

5.3. Rare earth element geochemistry

Table 5 gives abundances of REEs in the Föderata Group metacarbonates. The total REE concentrations are quite high, ranging from 13.56 to 49.62 ppm in the majority of samples, except for DP-5, DP-8, DP-9, DP-11, DP-12, DP-13, and DP-14 which have low concentrations. Most REEs from samples DP-8, DP-9, DP-11, DP-12, DP-13, and DP-14 are below the detection limits (Table 5). The tabulated

Table 4. Content of chosen trace elements in the Föderata Group metacarbonates compared with that in the sedimentary carbonate rocks.

Trace elements (ppm)	Föderata Group metacarbonates (this study)		Sedimentary carbonate rocks (Turekian and Wedepohl, 1961)	
	Mean	Range	Shallow sea (mean)	Deep sea (mean)
Ni	5.3	1.7–24.3	20.0	30.0
Zn	3.6	1.0–14.0	20.0	35.0
Sr	669.0	109.4–2683.0	610.0	2000.0
Mn	125.2	77.0–464.0	1100.0	1000.0

Table 5. Rare earth element composition (ppm) of metacarbonate rocks of the Föderata Group.

	T-1	T-2	T-3	T-4	T-5	T-6	T-7	T-8	R-1	R-2	PLD-1	PLD-2	PLD-3	PLD-4	PLD-5
La	12.6	7.1	9.3	10.0	14.3	10.8	9.6	15.4	13.5	18.9	8.1	7.4	9.5	11.7	2.9
Ce	6.3	4.5	7.5	4.3	7.6	5.9	5.0	6.9	4.6	5.8	11.8	11.0	9.3	10.1	5.7
Pr	2.53	1.37	1.79	1.70	3.07	1.98	1.91	3.46	2.63	3.28	1.78	1.64	2.06	2.72	0.66
Nd	11.5	5.8	6.5	6.7	12.3	7.9	7.9	13.7	11.0	12.9	7.2	6.5	7.8	10.9	2.6
Sm	1.85	1.02	1.09	1.22	2.02	1.34	1.36	2.38	1.72	2.15	1.42	1.30	1.45	2.10	0.44
Eu	0.44	0.22	0.26	0.28	0.44	0.30	0.31	0.50	0.37	0.52	0.37	0.35	0.30	0.50	0.08
Gd	1.72	0.92	1.05	1.21	1.82	1.27	1.31	2.02	1.69	2.13	1.49	1.56	1.40	2.23	0.36
Tb	0.24	0.15	0.15	0.17	0.26	0.18	0.20	0.26	0.25	0.31	0.28	0.26	0.23	0.35	0.05
Dy	1.29	0.71	0.94	0.91	1.43	0.86	0.90	1.31	1.20	1.55	1.48	1.57	1.26	1.96	0.33
Ho	0.25	0.17	0.17	0.21	0.29	0.18	0.20	0.31	0.25	0.34	0.34	0.32	0.26	0.39	0.05
Er	0.62	0.40	0.42	0.43	0.67	0.53	0.46	0.75	0.65	0.87	1.00	0.92	0.75	1.02	0.20
Tm	0.08	0.06	0.06	0.08	0.08	0.08	0.07	0.08	0.11	0.12	0.17	0.14	0.10	0.15	0.02
Yb	0.46	0.29	0.35	0.34	0.56	0.34	0.34	0.50	0.51	0.65	0.91	0.86	0.60	0.80	0.16
Lu	0.07	0.04	0.05	0.06	0.08	0.06	0.06	0.07	0.08	0.10	0.16	0.14	0.08	0.11	0.01
∑REE	39.95	22.75	29.63	27.61	44.92	31.72	29.62	47.64	38.56	49.62	36.50	33.96	35.09	45.03	13.56
∑LREE	35.22	20.01	26.44	24.20	39.73	28.22	26.08	42.34	33.82	43.55	30.67	28.19	30.41	38.02	12.38
∑HREE	4.73	2.74	3.19	3.41	5.19	3.50	3.54	5.30	4.74	6.07	5.83	5.77	4.68	7.01	1.18

Table 5. (Continued).

	DP-1	DP-2	DP-3	DP-4	DP-5	DP-6	DP-7	DP-8	DP-9	DP-10	DP-11	DP-12	DP-13	DP-14
La	5.5	4.5	5.4	6.7	1.5	6.0	5.7	0.6	1.0	6.3	0.9	1.3	1.3	0.3
Ce	5.3	4.5	6.2	6.7	2.8	4.3	4.8	1.0	1.8	5.3	1.2	1.8	1.7	0.4
Pr	1.12	0.91	1.11	1.37	0.35	1.11	1.09	0.12	0.22	1.21	0.15	0.22	0.23	0.07
Nd	4.1	3.8	4.3	5.3	1.0	4.4	4.5	0.5	0.9	4.7	0.5	1.0	0.9	<0.3
Sm	0.74	0.51	0.80	0.97	0.23	0.80	0.77	0.09	0.15	0.86	0.12	0.17	0.15	0.06
Eu	0.18	0.13	0.19	0.21	0.04	0.18	0.19	0.02	0.04	0.21	<0.02	<0.02	0.02	<0.02
Gd	0.71	0.59	0.80	0.98	0.21	0.87	0.92	0.08	0.18	0.99	0.06	0.10	0.14	<0.05
Tb	0.11	0.09	0.13	0.16	0.04	0.13	0.14	0.01	0.02	0.16	<0.01	<0.01	<0.01	<0.01
Dy	0.58	0.43	0.58	0.78	0.17	0.72	0.77	0.07	0.14	0.82	0.06	0.11	0.16	<0.05
Ho	0.14	0.09	0.13	0.18	0.04	0.17	0.17	<0.02	0.03	0.20	<0.02	<0.02	<0.02	<0.02
Er	0.36	0.22	0.35	0.46	0.10	0.44	0.43	0.04	0.06	0.52	<0.03	0.05	0.05	<0.03
Tm	0.04	0.03	0.05	0.07	0.02	0.06	0.06	<0.01	<0.01	0.08	<0.01	<0.01	<0.01	<0.01
Yb	0.25	0.20	0.30	0.38	0.11	0.32	0.34	<0.05	0.05	0.40	<0.05	<0.05	0.06	<0.05
Lu	0.04	0.03	0.04	0.06	0.02	0.04	0.04	<0.01	<0.01	0.07	<0.01	<0.01	<0.01	<0.01
∑REE	19.17	16.03	20.38	24.32	6.63	19.54	19.92	2.62	4.61	21.82	3.14	4.87	4.76	1.38
∑LREE	16.94	14.35	18.00	21.25	5.92	16.79	17.05	2.33	4.11	18.58	2.89	4.51	4.30	1.15
∑HREE	2.23	1.68	2.38	3.07	0.71	2.75	2.87	0.29	0.50	3.24	0.25	0.36	0.46	0.23

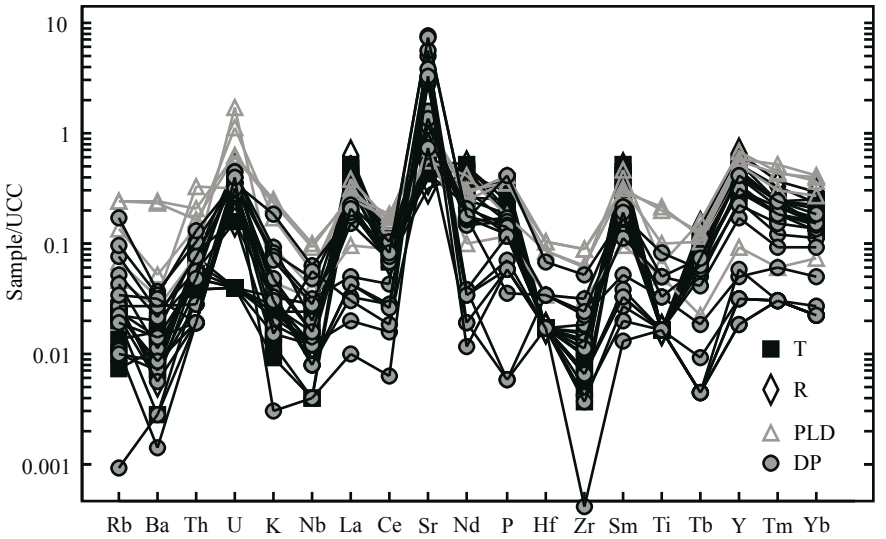

Figure 3. Multielement diagram of the Föderata Group metacarbonates normalized to the composition of the average upper continental crust (UCC). The elements are arranged from left to right in order of increasing compatibility in a small fraction melt of the mantle. The average UCC data are from Taylor and McLennan (1981).

data document that LREE components dominate over HREEs, and that total LREE and HREE concentrations decrease from 43.55 to 1.15 ppm and from 7.01 to 0.23 ppm, respectively (Table 5). It is likely that the high REE content of the Föderata Group metacarbonates is actually a result of the synmetamorphic infiltration or due to some post- or premetamorphic processes (Jarvis et al., 1975; Brilli et al., 2005). Identification of REE fractionation in the metacarbonate rocks studied was carried out by normalizing (Boynton, 1984) the concentration of the REEs to average chondritic meteorites and is presented as REE patterns (Figure 4). The chondrite-normalized REE

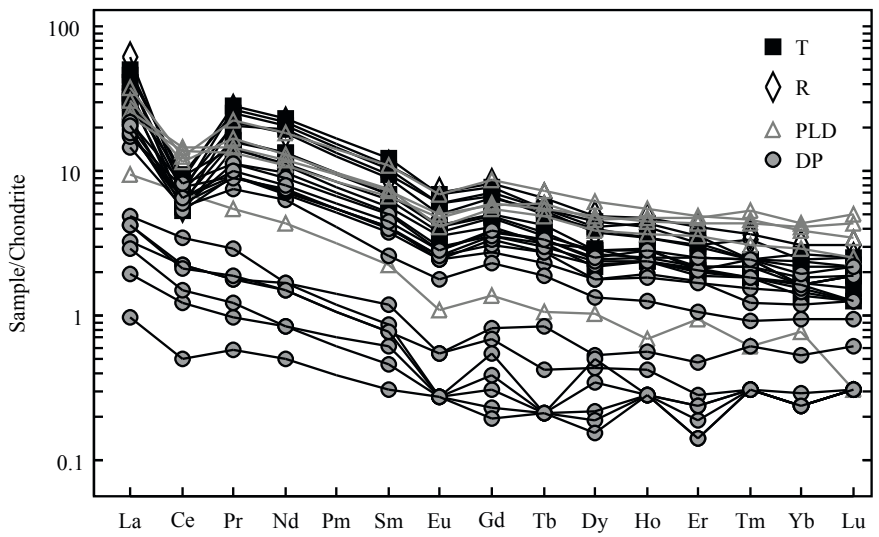

Figure 4. Chondrite-normalized REE diagram for metacarbonate samples from the Föderata Group. Note the similarity in the patterns with LREE enrichment, flat and uncoordinated zig-zag HREE distributions, and the ubiquitous negative Ce and Eu anomaly. REE chondrite-normalizing factors are from Boynton (1984).

plot shows relatively similar REE patterns for all samples, a moderate to strong fractionation of LREEs over HREEs (La_N/Yb_N = 4.05–21.42), and a distinct negative Ce and Eu anomaly, whereby Ce/Ce* ranges from 0.15 to 0.93 and Eu/Eu* varies from 0.42 to 1.09. It is also obvious that La – Pr – Nd – Sm – Eu define an inclined straight line and the HREEs exhibit uncoordinated zig-zag patterns in the Gd – Dy – Ho – Er – Yb – Lu spans (Figure 4). This peculiar type of REE distribution presumably also suggests the Föderata Group metacarbonates to have interacted with synmetamorphic fluids during the greenschist-facies metamorphism (Bağcı et al., 2010). Moreover, we attribute the negative Ce anomaly to climate warming and transgression conditions. According to Le Bas et al. (2002), we further argue that the negative Eu anomaly indicates carbonate rocks of sedimentary origin to be the protolith of the metacarbonates studied.

5.4. Geochemical interrelationships

The interrelationships between the major element oxides and trace elements of the Föderata Group metacarbonates are presented as covariation plots (Figures 5–9). Examination of changes of the major element oxides with respect to CaO concentration reveals that SiO_2 and MgO significantly decrease with increasing CaO content in the metacarbonates studied (Figure 5). The reduced SiO_2 content compared to increasing CaO concentration shows that the studied rocks comprise distinct silicate and carbonate fractions. The carbonate fraction increases at the expense of the silicate fraction and vice versa (Ephraim, 2012). CaO concentration also displays an expected negative correlation with TiO_2, Al_2O_3, Fe_2O_3, MnO, and K_2O (Figure 5). Furthermore, both MgO and Al_2O_3 are positively correlated with SiO_2 and there is no correlation between CaO and Na_2O (Figure 5). The positive relationship between SiO_2 and MgO most likely confirms earlier observations that parts of the silicate fraction are constituted by MgO. The noncarbonate fraction is dominated by aluminosilicates, as suggested by the positive relationship displayed between SiO_2 and Al_2O_3 and the negative correlation existing between CaO and the various insoluble residues. However, where Al_2O_3 is extremely low (as in samples DP-8 and DP-14), clearly the SiO_2 cannot have been introduced into the original sediment in aluminosilicate phases and was probably therefore either in traces of detrital quartz or in siliceous organisms, as speculated by Ephraim (2012).

Investigation of variations of trace elements in the metacarbonate rocks studied reveals that Sr is positively correlated with CaO values (Figure 6). Therefore, Sr appears to be enriched in the carbonate fractions. On the other hand, Pb, Ni, Cu, Ba, Nb, Rb, Zr, and Zn display a weak negative correlation with CaO (Figure 6) and hence these elements are concentrated in the silicate fractions. As stated above, in the Föderata Group metacarbonates, both Ca and Sr display very strong positive correlation, which suggests that both components are probably bound together in the same calcium-bearing lattice structures (Ephraim, 2012). This is consistent with Dissanayake (1981) that Sr as the main trace element in limestones and dolomites is often presumed to be located in the lattices of carbonate minerals. Based on the lack of significant positive correlation between Sr and Na (Figure 7), it was suggested that Na_2O is not controlled by the carbonate phases. Consequently, Na_2O does not form parts of the lattices of the Ca-Mg carbonates, nor does it occur as inclusions in the carbonate phases (Fritz and Katz, 1972; Land and Hoops, 1973). Due to the lack of strong relationship between Sr and Na, together with the absence of significant positive correlation between Na/Ca versus Mg/Ca or Sr/Ca (Figure 7), evaporitic hypersaline conditions (Sass and Katz, 1982) existing during developments of the protoliths of the Föderata Group metacarbonates can be precluded.

Interestingly, most trace elements exhibit positive interrelationships with the major insoluble residue components of the metacarbonates studied. The SiO_2 – Al_2O_3 – K_2O – TiO_2 – Ba – Nb – Rb – Zr links are among the most prominent (Figures 8 and 9). These strong positive interrelationships strengthen the relevance of the minor aluminosilicate phase in controlling the distribution of both insoluble components and most trace elements (Ephraim, 2012). Accordingly, the positive correlation among Al_2O_3 and TiO_2, K_2O, Ba, Nb, Rb, and Zr (Figures 8 and 9) indicates that all these components are contained in different proportions of aluminosilicate phases. The strong positive interrelationship among Ba, Rb, and K_2O (Figures 8 and 9) supports the relevance of K-bearing minerals in the aluminosilicate phases (Ephraim, 2012). For a long time, it has been known that Ba and Rb are especially contained in K-bearing minerals, and feldspars are among the most common K-bearing minerals. However, the nonlinear interrelationships involving Na, Pb, Sr, and Al_2O_3 (Figure 7) and Na_2O and CaO (Figure 5) corroborate petrographic observations (Table 1 and Ružička et al., 2011) that feldspar does not constitute the significant phase in the mineralogy of metacarbonates from the Föderata Group; rather, quartz, muscovite, phlogopite, illite, and kaolinite are the main aluminosilicate phases in these rocks.

5.5. C, O, and Sr isotope composition

The C-, O-, and Sr-isotopic data of the Föderata Group metacarbonates are presented in Table 6. The $\delta^{13}C_{PDB}$ values fluctuate from marginally positive (2.36‰) to negative (–3.34‰). The $\delta^{18}O_{PDB}$ values for the analyzed Föderata Group metacarbonate samples range from –9.39‰ to –2.63‰. The $^{87}Sr/^{86}Sr$ ratios lie between 0.707513 and 0.708051. The C- and O-isotopic characteristics of the Föderata Group metacarbonates are illustrated in the

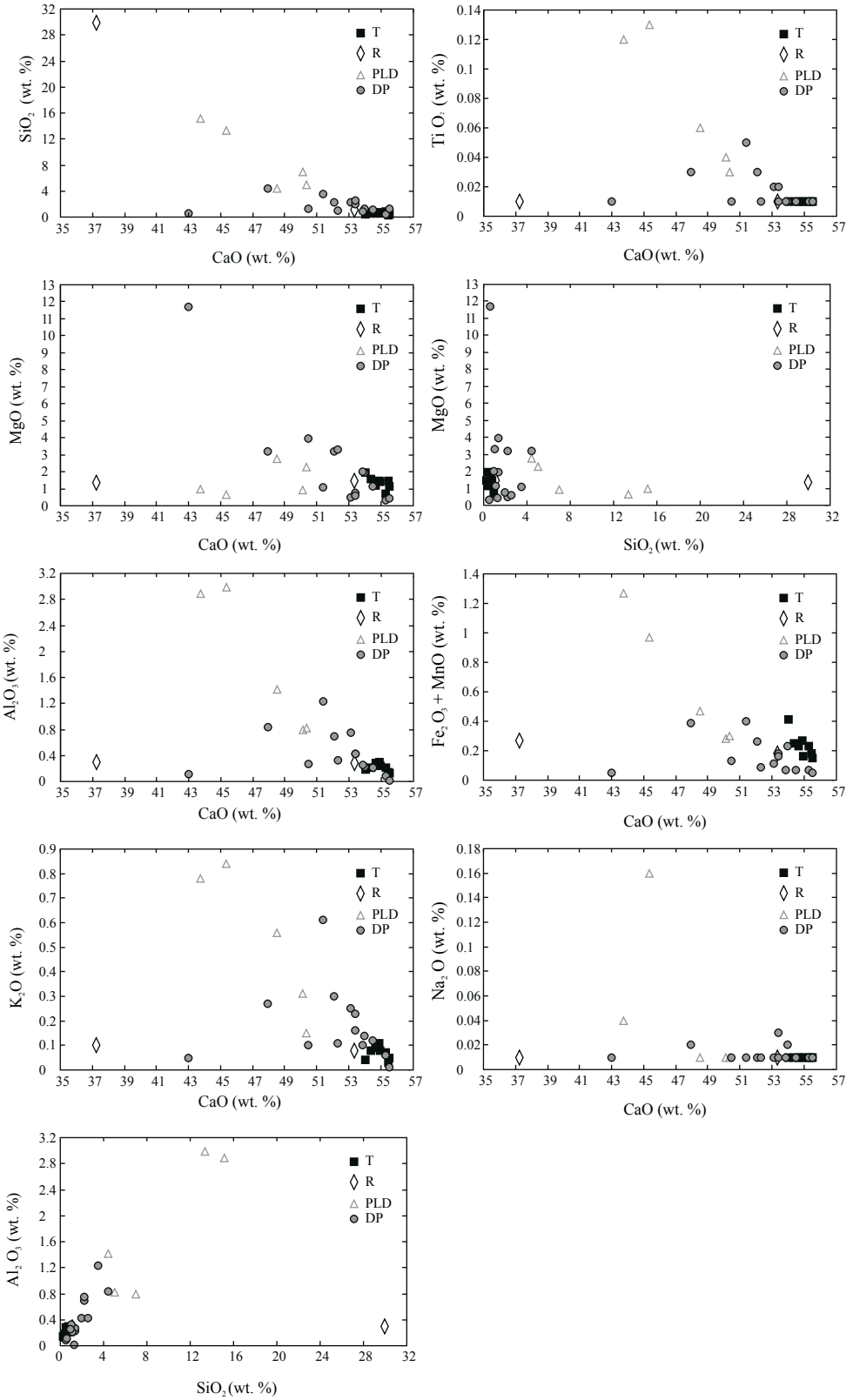

Figure 5. The degree of correspondence between the major element oxides of the metacarbonates studied.

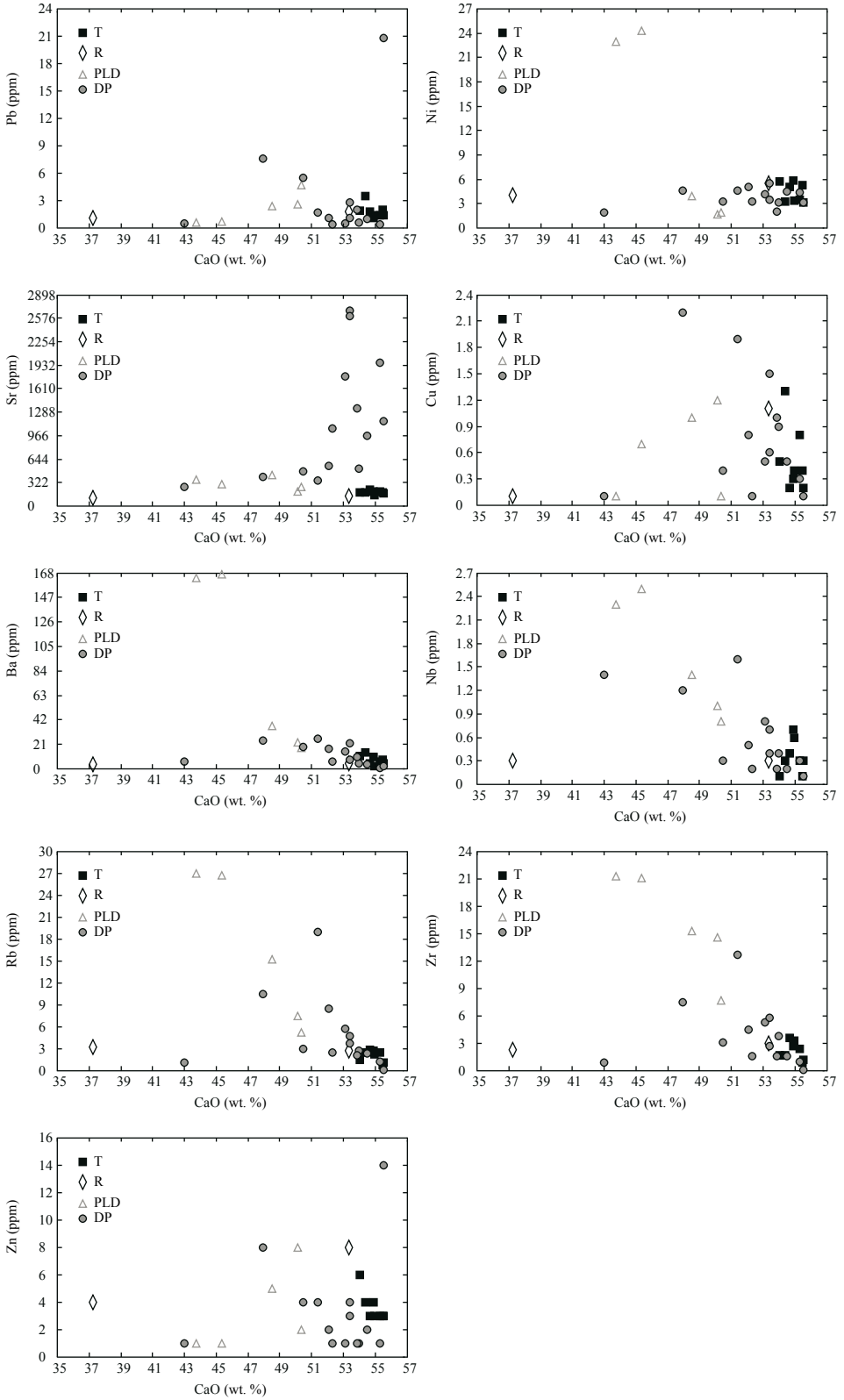

Figure 6. The degree of correspondence of selected trace elements with CaO composition of the Föderata Group metacarbonates.

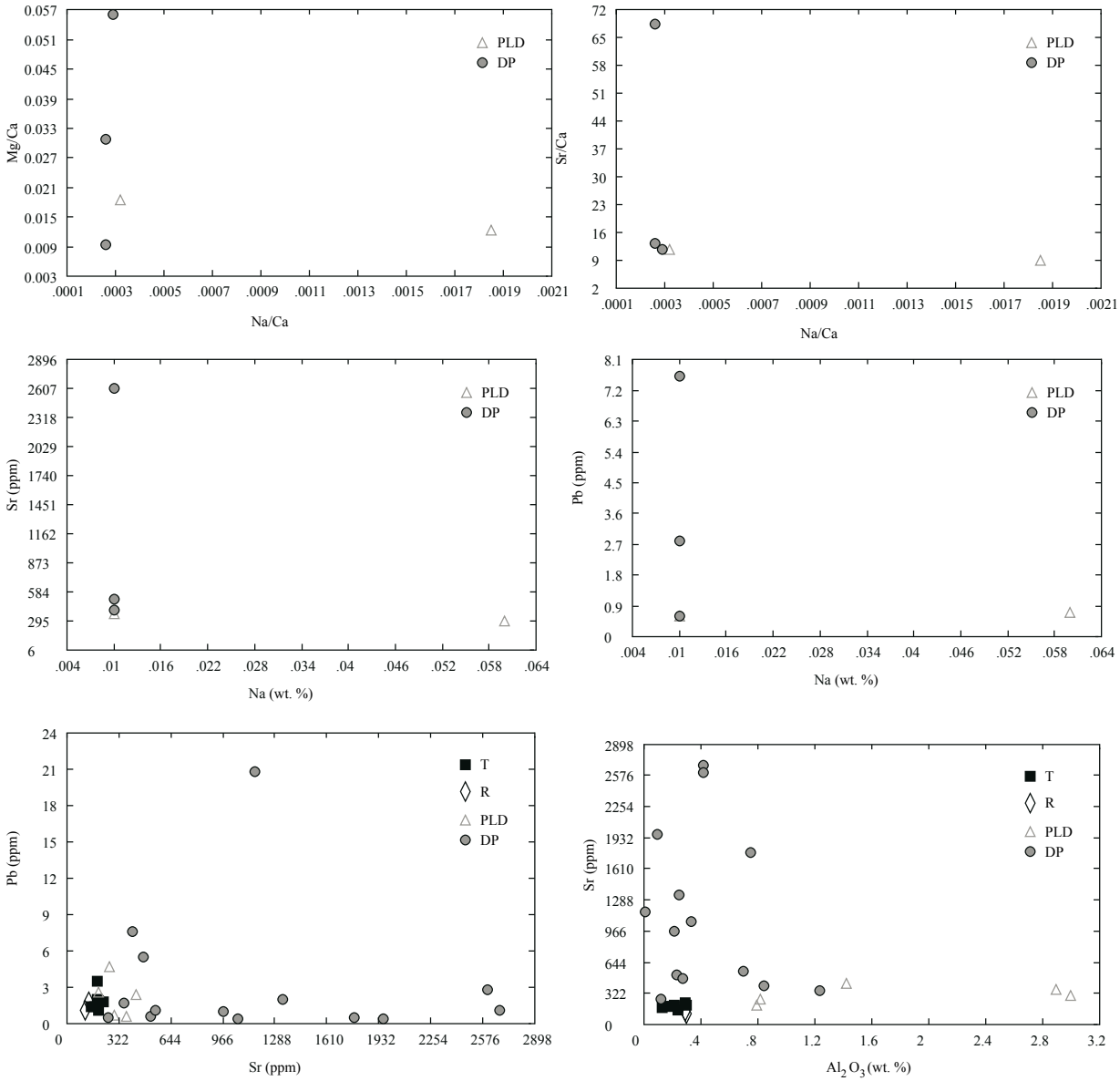

Figure 7. Cross-plots showing vague and inconsistent interrelationships displayed among various chemical components of the Föderata Group metacarbonate rocks.

conventional $\delta^{18}O$–$\delta^{13}C$ cross-plot (Figure 10). A narrow range of the $\delta^{18}O$ and $\delta^{13}C$ values indicates a more or less homogeneous dataset.

The original isotopic signatures of carbonate rocks can be altered by a number of postdepositional processes, beginning with the early diagenesis and dolomitization. Therefore, it is necessary to assess the data before attempting an interpretation of the depositional conditions (e.g., Pandit et al., 2009). Various geochemical parameters have been proposed for evaluation of the degree of preservation of primary isotopic signatures (Veizer, 1983; Kaufman et al., 1993; Narbonne et al., 1994). However, none of the suggested parameters are independently conclusive. For instance, Narbonne et al. (1994) identified enrichment in Fe and Mn and depletion in Sr as useful indicators for evaluating the diagenetic history in successor phases. Indeed, according to Brand and Veizer (1980), the degree of alteration and postdepositional modifications is reliably assessed by the Mn/Sr ratio. Samples with Mn/Sr ratio of <3 are considered to be well preserved and unaffected by postdepositional alterations (Derry et al., 1992), but values as high as 10 are also found acceptable and being little affected by postdepositional processes (Veizer, 1983). A nonlinear Mn/Sr–$\delta^{13}C_{PDB}$ (Figure 11a) relationship

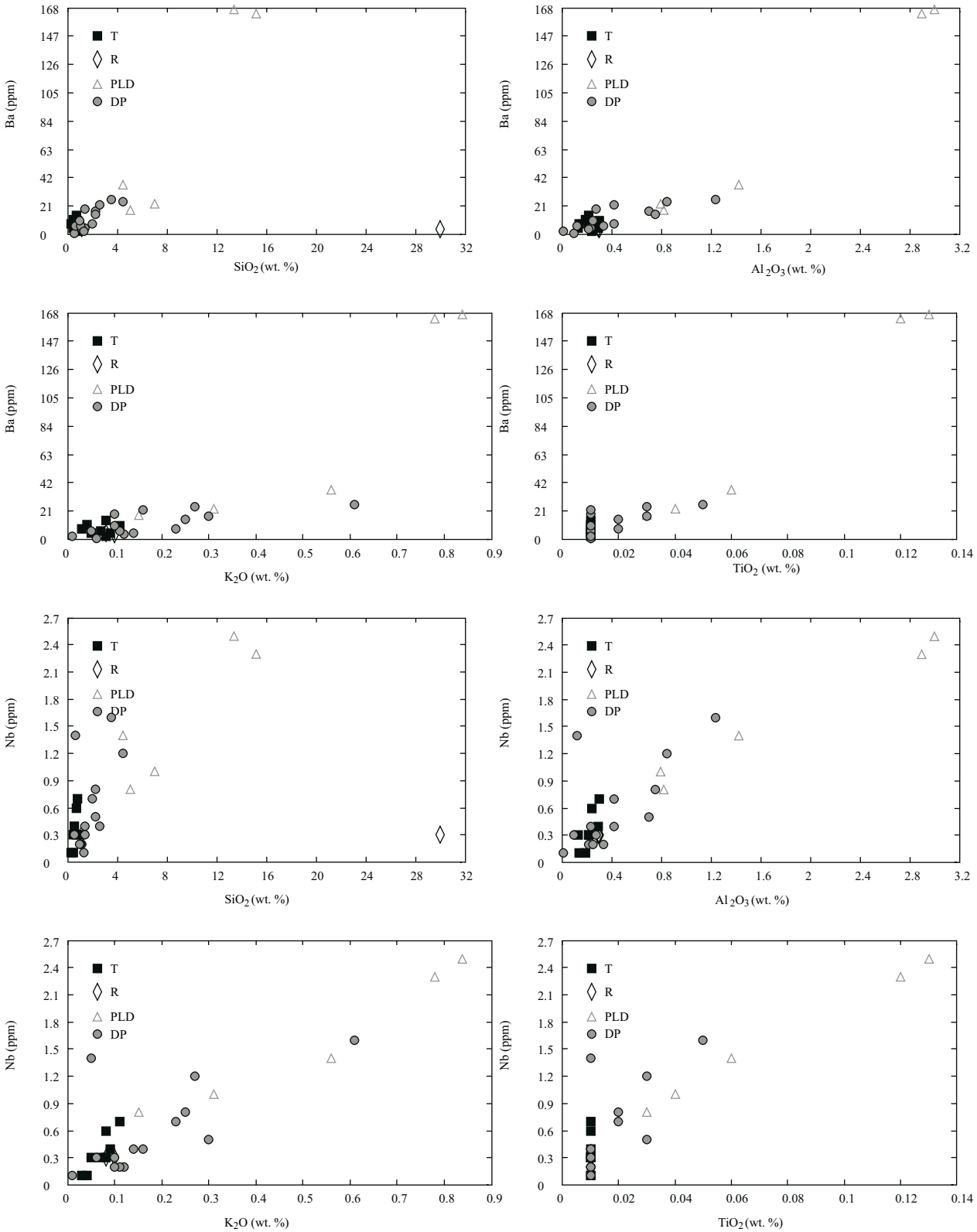

Figure 8. Cross-plots showing the varying degrees of positive interrelationships displayed between various trace elements and the insoluble residue components of the Föderata Group metacarbonates.

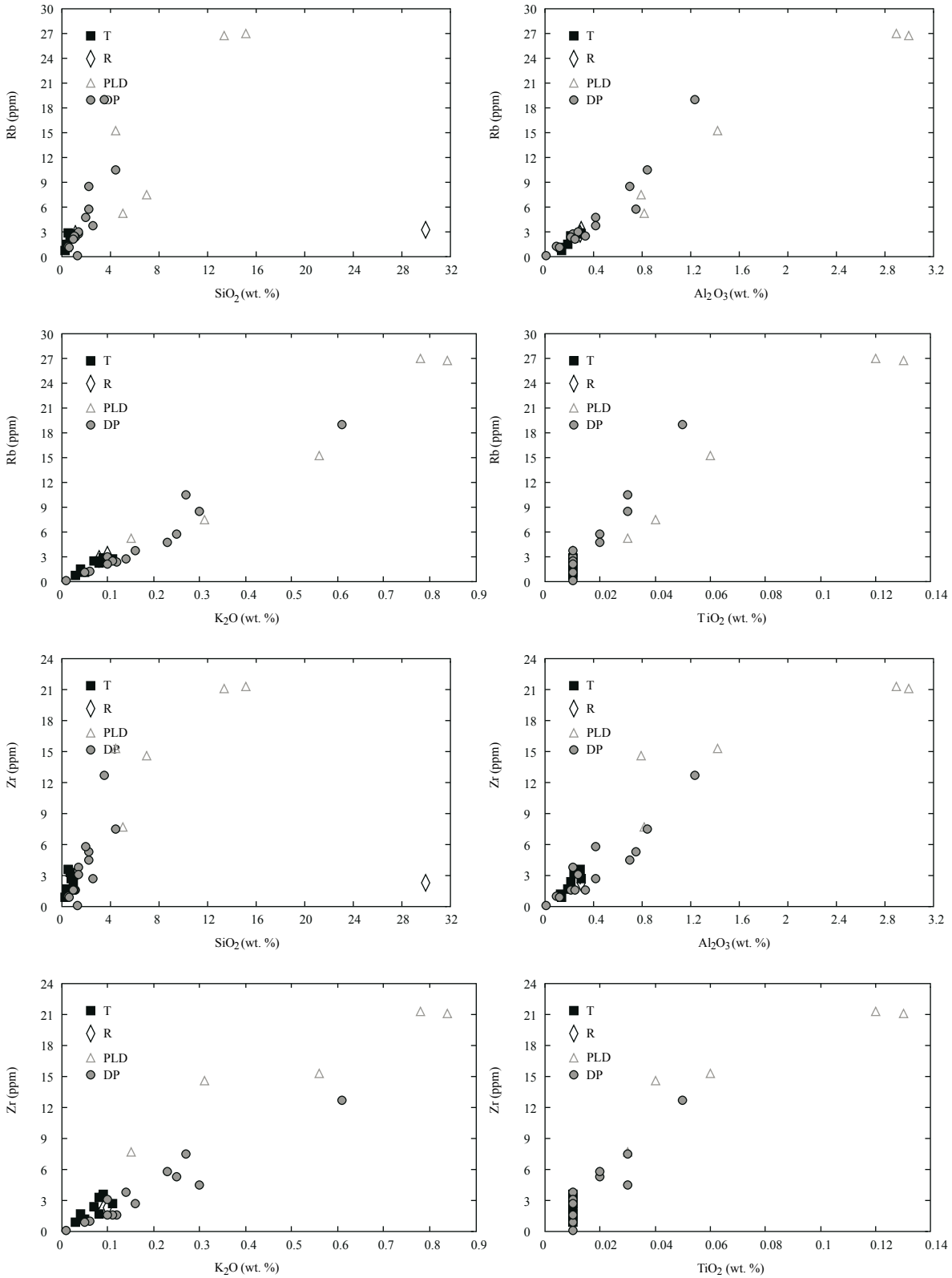

Figure 9. Cross-plots showing the varying degrees of positive interrelationships displayed between various trace elements and the insoluble residue components of the Föderata Group metacarbonates.

Table 6. Isotopic composition of the Föderata Group metacarbonates. C- and O-isotopic compositions are represented as standard δ‰ notation relative to PDB and V-SMOW. Errors in measurements of Sr isotopes are expressed as 2σ values.

Sample	$\delta^{13}C_{PDB}$	$\delta^{18}O_{PDB}$	$\delta^{18}O_{SMOW}$	CO_2	$^{87}Sr/^{86}Sr \pm 2\sigma$
T-1	2.04	–4.23	26.50	43.30	n.a.
T-2	2.36	–3.37	27.38	42.59	n.a.
T-3	1.64	–5.82	24.86	42.59	0.708051 ± 0.000010
T-4	2.24	–3.76	26.99	41.54	n.a.
T-5	1.24	–7.61	23.02	41.54	n.a.
T-6	1.98	–5.34	25.35	41.18	0.707968 ± 0.000008
T-7	1.97	–4.93	25.78	41.54	n.a.
T-8	1.74	–4.31	26.42	41.89	n.a.
R-1	1.47	–2.87	27.91	32.05	0.707768 ± 0.000010
R-2	1.56	–2.63	28.15	42.83	0.707513 ± 0.000014
PLD-1	–1.54	–9.04	21.54	34.32	n.a.
PLD-2	–3.34	–8.94	21.64	35.38	n.a.
PLD-3	0.57	–6.09	24.58	40.22	n.a.
PLD-4	0.22	–6.34	24.33	41.65	n.a.
PLD-5	–0.43	–7.99	22.63	35.35	n.a.
DP-1	1.16	–7.00	23.65	40.48	n.a.
DP-2	1.63	–6.23	24.44	40.13	n.a.
DP-3	0.14	–7.81	22.81	35.97	n.a.
DP-4	1.04	–8.29	22.31	38.43	n.a.
DP-5	1.98	–8.34	22.27	38.43	n.a.
DP-6	1.09	–8.51	22.08	42.09	n.a.
DP-7	0.98	–8.68	21.91	40.26	0.707806 ± 0.000018
DP-8	2.17	–8.13	22.48	41.36	n.a.
DP-9	2.08	–9.39	21.20	39.16	n.a.
DP-10	0.82	–7.62	23.00	42.83	0.707824 ± 0.000011
DP-11	1.16	–9.30	21.27	46.46	n.a.
DP-12	1.47	–8.84	21.74	44.26	n.a.
DP-13	1.24	–8.77	21.82	44.26	n.a.
DP-14	2.32	–8.20	22.41	43.16	n.a.

n.a. = Not analyzed.

indicates that the metacarbonate samples studied are generally unaffected by postdepositional alterations, which would have otherwise resulted in depletion of $\delta^{13}C$ and in a corresponding increase in the Mn/Sr ratio (Kaufman and Knoll, 1995). Another useful parameter is the Mg/Ca ratio, whereby a simultaneous increase in the Mg/Ca and Mn/Sr ratios can be attributed to the alteration process (Kaufman and Knoll, 1995). A nonlinear relationship existing between these two parameters in the Mg/Ca–Mn/Sr cross-plot (Figure 11b) precludes any notable alteration effect. An indistinctive positive correlation of Mg/Ca with both $\delta^{18}O$ and $\delta^{13}C$ (Figures 11c and 11d) is also consistent with unaltered isotopic and geochemical signatures (Melezhik et al., 2001).

On the basis of the above, the C-isotopic data of the Föderata Group metacarbonates can be considered to be pristine and representative of the original isotopic ratios. Therefore, the isotopic signatures can be found as representative of the seawater. For a given element at the time of diagenetic recrystallization, the isotopic

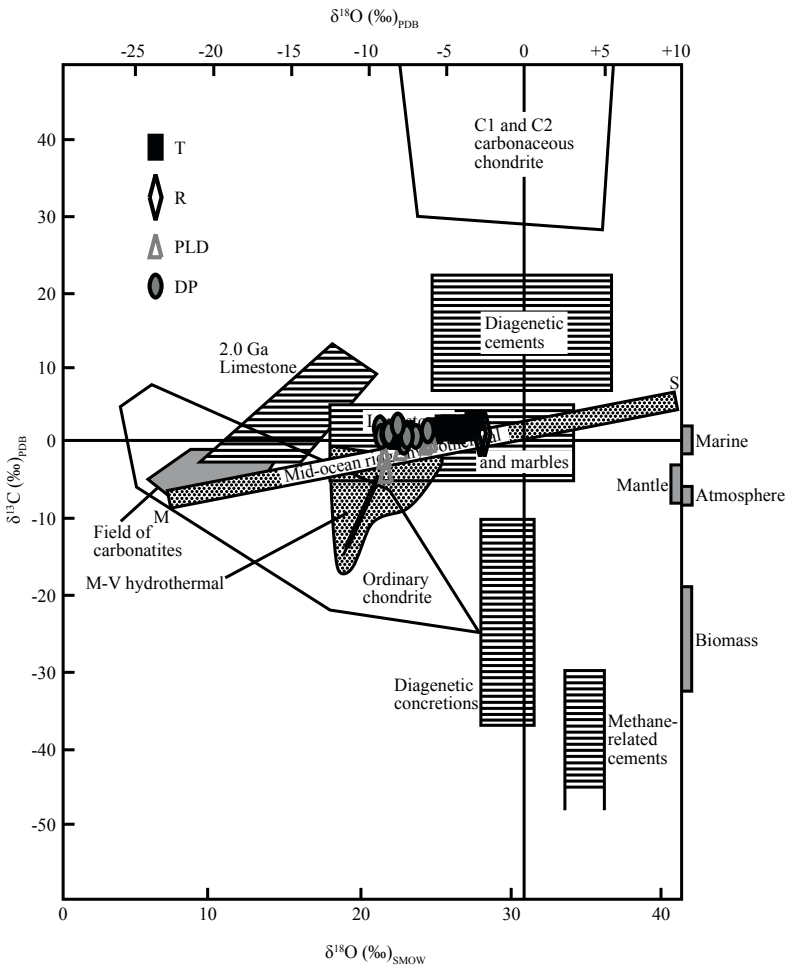

Figure 10. $\delta^{18}O$ versus $\delta^{13}C$ plot showing the composition of the Föderata Group metacarbonates and carbonates from a variety of environments (after Rollinson, 1993). $\delta^{18}O$ is plotted relative to both the SMOW and PDB scales. The isotopic composition of a number of different carbon reservoirs is plotted along the right-hand side of the diagram. The values for sedimentary carbonates (horizontal rule) are from Hudson (1977) and Baker and Fallick (1989); hydrothermal calcites (stippled ornament) from the midocean ridges show mixing between mantle-derived carbon (M) and seawater carbon (S) (Stakes and O'Neil, 1982); in the field of hydrothermal calcites from Mississippi Valley-type deposits (M-V hydrothermal) the arrow shows the direction of younging (Richardson et al., 1988). Chondrite compositions (unornamented) are from Wright et al. (1988). The field of carbonatites is from Deines and Gold (1973).

signature preservation depends on the water/rock ratio (Burdett et al., 1990). The reported sequence of water–rock interaction is O > Sr > C, showing that the C-isotopic values are the least modified. At elevated temperatures during metamorphism, circulating meteoric waters generally more likely affect oxygen isotopes. Carbonates with the $\delta^{18}O$ range of –10‰ to –5‰ can be considered as primary (Pandit et al., 2009). Thus, the $\delta^{18}O$ values for the Föderata Group metacarbonates (Table 6) suggest that the O-isotopic signatures have not been modified.

Likewise, the correlation between $\delta^{13}C$ and $\delta^{18}O$ (Figure 10) indicates well-preserved primary signatures in the metacarbonates studied. Due to devolatilization reactions, late diagenesis, and low-grade metamorphism as well as deformation would result in a corresponding lowering of both $\delta^{13}C$ and $\delta^{18}O$ values. Therefore, we conclude that the $\delta^{13}C$ values close to zero (±2‰) are indicative of warmer climatic conditions during deposition of the Föderata Group carbonate rocks. Marginally negative $\delta^{13}C$ values, observed in some cases, can be attributed to the

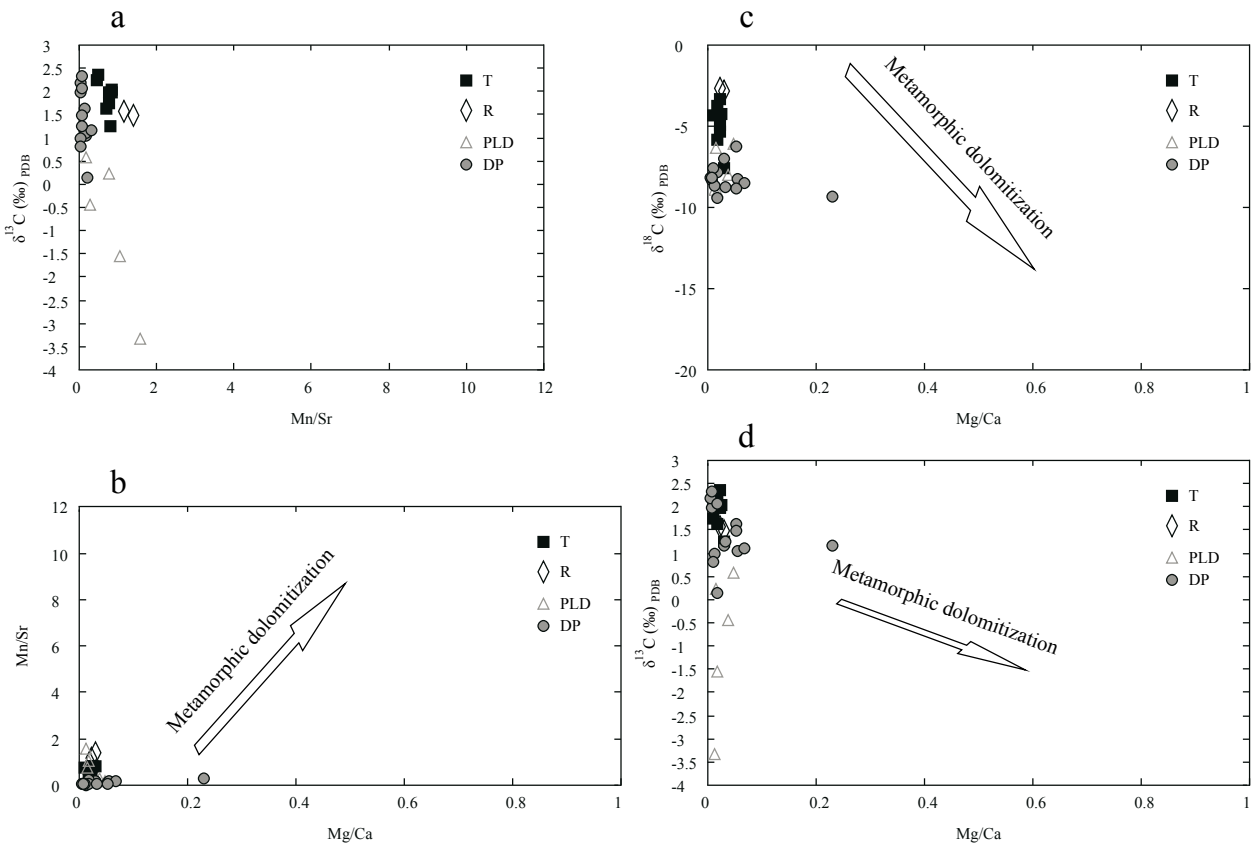

Figure 11. Variation in some diagnostic geochemical parameters and C- and O-isotopic characteristics of the Föderata Group metacarbonates, indicating that the geochemical and isotopic signatures have not been significantly modified during postdepositional processes. Known trends of metamorphic dolomitization (after Pandit et al., 2001) have also been superimposed. (a) Mn/Sr–$\delta^{13}C$ variation. (b) Mg/Ca–Mn/Sr variation. (c) Mg/Ca variation against $\delta^{18}O$. (d) Mg/Ca variation against $\delta^{13}C$.

metamorphic decarbonation reactions that also reduce these values.

$^{87}Sr/^{86}Sr$ ratios in the Föderata Group metacarbonates were compared with data from various world localities using the study of Koepnick et al. (1990) (Figure 12). The authors evaluated 128 $^{87}Sr/^{86}Sr$ values in samples from 18 states and countries in North America, Europe, Africa, and Asia and constructed a plot of $^{87}Sr/^{86}Sr$ versus age for the Late Permian, Triassic, Jurassic, and Early Cretaceous. Furthermore, they defined a band that encloses 90% of the analyzed data points. Their estimate of the actual seawater ratio as a function of time is shown as a line within this band. Samples from Ružiná have the lowest $^{87}Sr/^{86}Sr$ values, with one data point situated at the lower line of the band and the other data point near the estimated seawater line in the center of the band. Samples from the Dobšiná Brook valley are also plotted in the midband, but slightly above the Ružiná samples. Finally, Tuhár samples with the highest $^{87}Sr/^{86}Sr$ ratio are depicted slightly above the upper seawater line (Figure 12), which might be a result of metamorphic processes that could have influenced the redistribution of Rb and Sr. Since our data points plot within or nearby the band, we consider the Föderata Group metacarbonates to have a marine origin.

5.6. Conditions of formation of the Föderata Group metacarbonates

In an effort to gain insight into the premetamorphic conditions of the parent materials of the Föderata Group metacarbonates, the chemical data of these rocks were plotted on the Na_2O/Al_2O_3 versus K_2O/Al_2O_3 diagram (according to Garrels and Mackenzie, 1971) and the $MgO–CaO–Al_2O_3$ discrimination diagram (according to Leyreloup et al., 1977). The metacarbonate samples were exclusively plotted in the sedimentary field of the Na_2O/Al_2O_3 versus K_2O/Al_2O_3 diagram (Figure 13), thereby confirming the sedimentary origin of the Föderata Group metacarbonates. On the $MgO–CaO–Al_2O_3$ discrimination diagram (Figure 14), the metacarbonate rock samples were plotted outside the magmatic funnel, thereby supporting the sedimentary antecedents of the Föderata Group metacarbonates. In addition, the SiO_2 – Al_2O_3 – K_2O – TiO_2 – Ba – Nb – Rb – Zr links (Figures 8 and 9) hint

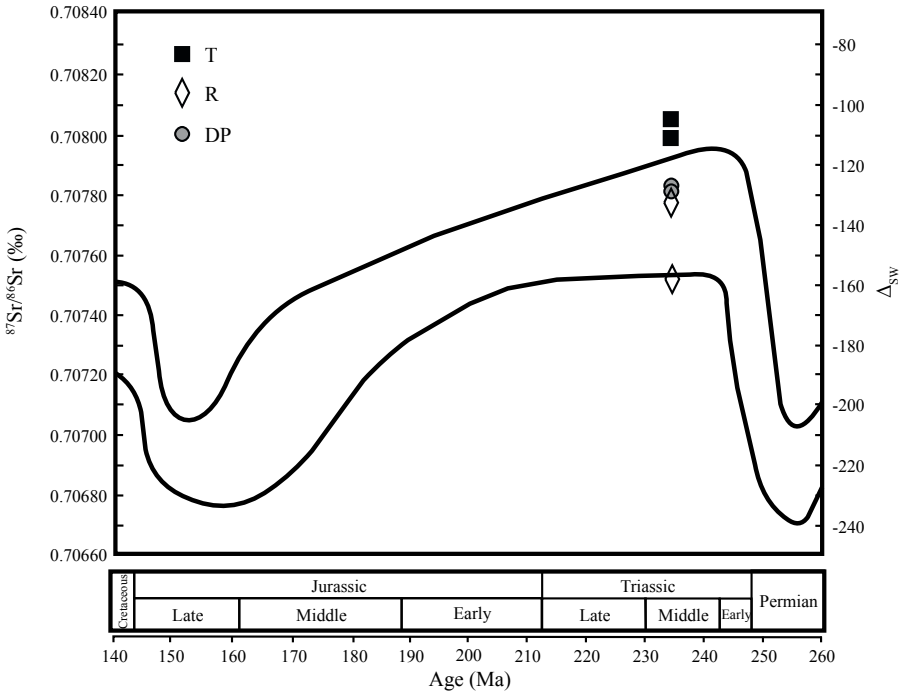

Figure 12. Distribution of $^{87}Sr/^{86}Sr$ ratios from the Permian to the Cretaceous, with superimposed range of the curve of seawater (after Koepnick et al., 1990). $^{87}Sr/^{86}Sr$ ratio values of the Föderata Group metacarbonates are plotted onto this diagram.

at a close association of the parent carbonate rocks with aluminosilicate phases, which is a diagnostic sedimentary feature.

The nature and characteristics of the depositional environment of the parent sedimentary carbonate were investigated using the trace element and especially REE composition. According to Tanaka and Kawabe (2006), unaltered marine sedimentary carbonates should have preserved the chemical characteristics (i.e. REE features) of the medium in which they precipitated. However, since carbonate REE content could also be influenced by noncarbonate materials, such as fine-grained siliciclastic material in excess of 5% (Banner et al., 1988), great care must be taken when making such an interpretation. Fortunately, petrographic and geochemical observations have shown that noncarbonate phases are negligible in the analyzed Föderata Group metacarbonates and hence an additional influence on the REE chemistry of the studied rocks by noncarbonates can be excluded.

Tanaka et al. (1990) recognized differences in REE patterns between shallow coastal waters and deep waters. Specifically, in the case of coastal waters, data points for La, Nd, Sm, and Eu fall on a nearly straight line and the REE patterns are characterized by marked discontinuity between Eu and Gd. Similar observations have been made for the REE pattern of the Föderata Group metacarbonates (Figure 4), which suggests that the protoliths of these rocks were deposited in a shallow, near-shore marine environment.

Besides, the observed uncoordinated zig-zag patterns in the Gd – Dy – Ho – Er – Yb – Lu spans of the HREEs of the Föderata Group metacarbonates (Figure 4) require further investigation, because such features can also be related to a surface or shallow water environment (Masuda and Ikeuchi, 1979; Tanaka et al., 1990). Determination of a surface or shallow marine depositional environment for the parent carbonate material of the Föderata Group metacarbonates is in agreement with the reported negligible Na_2O, Fe_2O_3, and MnO concentrations (Table 2) (Clarke, 1911; Turekian and Wedepohl, 1961; Frank, 1975). According to Ikhane et al. (2009), we consider the low Al_2O_3 concentration in the Föderata Group metacarbonates as an indication of a low-energy environment.

6. Conclusions

The Föderata Group metacarbonates from the SVU Mesozoic cover sequence comprised distinct carbonate and minor silicate fractions. While the carbonate fraction includes Ca, Mg, and Sr, the silicate fraction is associated with Si, Al, K, Ti, Pb, Ni, Cu, Ba, Nb, Rb, Zr, and Zn. Geochemical data, integrated with the C-, O-, and Sr-isotopic data, have been used to infer a metasedimentary petrogenetic affiliation for the studied rocks. The Föderata Group metacarbonates were very likely formed from

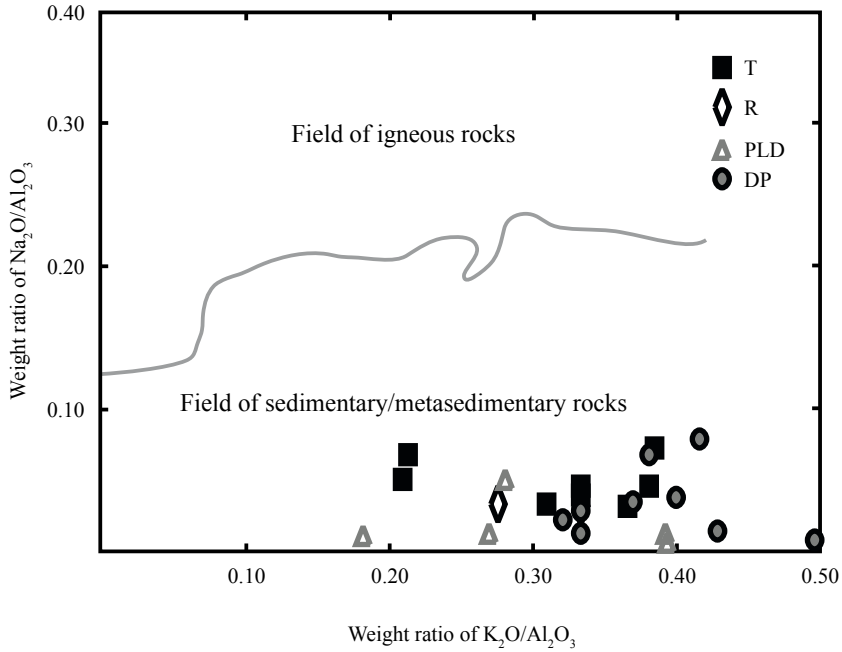

Figure 13. Composition of the Föderata Group metacarbonate rocks on the Na_2O/Al_2O_3 versus K_2O/Al_2O_3 discrimination diagram of Garrels and Mackenzie (1971).

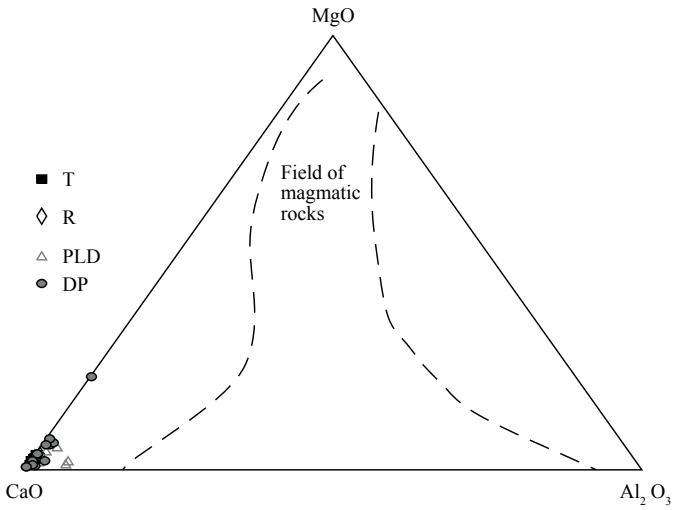

Figure 14. Composition of the Föderata Group metacarbonate rocks on the MgO–CaO–Al_2O_3 diagram by Leyreloup et al. (1977).

sedimentary carbonate materials that were deposited in a saline, shallow-marine, low-energy environment. The negative Ce anomaly and the $\delta^{13}C$ values indicate warmer climatic conditions during deposition. In general, the consistency in the chemical properties of the metacarbonate rocks studied most likely reflects relative stability during deposition of the initial sediments.

Acknowledgments
This work was supported by the Slovak Research and Development Agency under Contracts No. APVV-0438-06, APVV-0546-11, and APVV-14-0118. Further financial support came from the Grant Agency of the Ministry of Education, Science, Research, and Sport of the Slovak Republic and Slovak Academy of Sciences (VEGA No. 2/0034/16).

References

Bağcı M, Kibici Y, Yıldız A, Akıncı ÖT (2010). Petrographical and geochemical investigation of the Triassic marbles associated with Menderes massif metamorphics, Kavaklıdere, Muğla, SW Turkey. J Geochem Explor 107: 39-55.

Baker AJ, Fallick AE (1989). Evidence from Lewisian limestones for isotopically heavy carbon in two-thousand-million-year-old sea water. Nature 337: 352-354.

Banner JL, Hanson GN, Meyers WJ (1988). Water-rock interaction history of regionally extensive dolomites of the Burlington-Keokuk Formation (Mississippian): isotopic evidence. In: Shukla V, Baker PA, editors. Sedimentology and Geochemistry of Dolostones. Tulsa, OK, USA: Society of Economic Paleontologists and Mineralogists, pp. 97-113.

Biely A, Bezák V, Elečko M, Gross P, Kaličiak M, Konečný V, Lexa J, Mello J, Nemčok J, Potfaj M et al. (1996). Explanations to the Geological Map of Slovakia 1:500 000. Bratislava, Slovakia: State Geological Institute of Dionýz Štúr.

Biely A, Planderová E (1975). On Triassic age of the limestones from the cover Veporic unit (Struženík area). Geol Práce Spr 63: 91-93 (in Slovak).

Böttcher ME (1996). $^{18}O/^{16}O$ and $^{13}C/^{12}C$ fractionation during the reaction of carbonates with phosphoric acid: effects of cationic substitution and reaction temperature. Isot Environ Health Stud 32: 299-305.

Boynton RS (1980). Chemistry and Technology of Lime and Limestone. New York, NY, USA: John Wiley and Sons Inc.

Boynton WV (1984). Geochemistry of the rare earth elements: meteorite studies. In: Henderson P, editor. Rare Earth Element Geochemistry. Amsterdam, the Netherlands: Elsevier, pp. 63-114.

Brand U, Veizer J (1980). Chemical diagenesis of a multicomponent carbonate system--1: Trace elements. J Sediment Petrol 50: 1219-1236.

Brilli M, Cavazzini G, Turi B (2005). New data of $^{87}Sr/^{86}Sr$ ratio in classical marble: an initial database for marble provenance determination. J Archaeol Sci 32: 1543-1551.

Brownlow AH (1996). Geochemistry. 2nd ed. Trenton, NJ, USA: Prentice Hall.

Burdett JW, Grotzinger JP, Arthur MA (1990). Did major changes in the stable-isotope composition of Proterozoic seawater occur? Geology 18: 227-230.

Carothers WW, Adami LH, Rosenbauer RJ (1988). Experimental oxygen isotope fractionation between siderite-water and phosphoric acid liberated CO_2-siderite. Geochim Cosmochim Acta 52: 2445-2450.

Clarke FW (1911). The Data of Geochemistry. 2nd ed. Washington, DC, USA: Washington Government Printing Office.

Clarke FW (1924). The Data of Geochemistry. 5th ed. Washington, DC, USA: Washington Government Printing Office.

Deines P, Gold DP (1973). The isotopic composition of carbonatite and kimberlite carbonates and their bearing on the isotopic composition of deep-seated carbon. Geochim Cosmochim Acta 37: 1709-1733.

Derry LA, Kaufman AJ, Jacobsen SB (1992). Sedimentary cycling and environmental change in the Late Proterozoic: evidence from stable and radiogenic isotopes. Geochim Cosmochim Acta 56: 1317-1329.

Dissanayake CB (1981). The strontium geochemistry of some Precambrian carbonate rocks of Sri Lanka. J Natn Sci Coun Sri Lanka 9: 255-267.

Ephraim BE (2012). Investigation of the geochemical signatures and conditions of formation of metacarbonate rocks occurring within the Mamfe embayment of south-eastern Nigeria. Earth Sci Res J 16: 121-138.

Frank W (1975). Sediment Chemische and Palolcologische Asperkte Stablier Schewellen. Ben Sonderforschungsberoich 48. Göttingen, Germany: University of Göttingen (in German).

Friedman I, O'Neil JR (1977). Compilation of Stable Isotope Fractionation Factors of Geochemical Interest. Geological Survey Professional Paper 440-KK. Washington, DC, USA: US Geological Survey.

Fritz P, Katz A (1972). The sodium distribution of dolomite crystals. Chem Geol 10: 237-244.

Garrels RM, Mackenzie FT (1971). Evolution of Sedimentary Rocks. New York, NY, USA: WW Norton and Company Inc.

Georgieva M, Cherneva Z, Hekimova S, Petrova A (2009). Petrology of marbles from the Arda tectonic unit, Central Rhodope, Bulgaria. In: Proceedings of National Conference "Geosciences 2009", pp. 43-44.

Hók J, Kahan Š, Aubrecht R (2001). Geology of Slovakia. Bratislava, Slovakia: Comenius University in Bratislava.

Hudson JD (1977). Stable isotopes and limestone lithification. J Geol Soc London 133: 637-660.

Ikhane PR, Folorunso AF, Nton ME, Oluwalaanu JA (2009). Evaluations of Turonian limestone formation exposed at NIGERCEM-Quarry, Nkalagu, southeastern Nigeria: a geochemical approach. Pac J Sci Technol 10: 763-771.

Jarvis JC, Wildeman TR, Banks NG (1975). Rare earths in the Leadville Limestone and its marble derivates. Chem Geol 16: 27-37.

Johnson CA, Taylor CD, Leventhal JS, Freitag K (2010). Geochemistry of metasedimentary rocks in the hanging wall of the greens creek massive sulfide deposit and of shales elsewhere on Admiralty Island. In: Taylor CD, Johnson CA, editors. Geology, Geochemistry, and Genesis of the Greens Creek Massive Sulfide Deposit, Admiralty Island, Southeastern Alaska. US Geological Survey Professional Paper 1763. Washington, DC, USA: US Geological Survey, pp. 159-182.

Kaufman AJ, Jacobsen SB, Knoll AH (1993). The Vendian record of Sr and C isotopic variations in seawater: Implications for tectonics and paleoclimate. Earth Planet Sci Lett 120: 409-430.

Kaufman AJ, Knoll AH (1995). Neoproterozoic variations in the C-isotopic composition of seawater: stratigraphic and biogeochemical implications. Precambrian Res 73: 27-49.

Koepnick RB, Denison RE, Burke WH, Hetherington EA, Dahl DA (1990). Construction of the Triassic and Jurassic portion of the Phanerozoic curve of seawater $^{87}Sr/^{86}Sr$. Chem Geol (Isot Geosci Sect) 80: 327-349.

Krauskopf KB, Bird DK (1995). Introduction to Geochemistry. 3rd ed. New York, NY, USA: McGraw-Hill.

Land LS, Hoops GK (1973). Sodium in carbonate sediments and rocks: A possible index to the salinity of diagenetic solutions. J Sediment Petrol 43: 614-617.

Le Bas MJ, Subbarao KV, Walsh JN (2002). Metacarbonatite or marble? – The case of the carbonate, pyroxenite, calcite–apatite rock complex at Borra, Eastern Ghats, India. J Asian Earth Sci 20: 127-140.

Leyreloup A, Dupuy C, Andriambololona R (1977). Catazonal xenoliths in French Neogene volcanic rocks: constitution of the lower crust. 2. Chemical composition and consequences of the evolution of the French Massif Central Precambrian crust. Contrib Mineral Petrol 62: 283-300.

Madarás J, Hók J, Kováč P, Mello J, Ivanička J, Vozár J, Vozárová A, Hraško Ľ, Lexa O, Kucharič Ľ et al. (1995). Geological and Structural Analysis of the Contact Zone of the Gemeric and Veporic Unit. Bratislava, Slovakia: State Geological Institute of Dionýz Štúr.

Masuda A, Ikeuchi Y (1979). Lanthanide tetrad effect observed in marine environment. Geochem J 13: 19-22.

McCrea JM (1950). On the isotopic chemistry of carbonates and a paleotemperature scale. J Chem Phys 18: 849-857.

Melezhik VA, Gorokhov IM, Fallick AE, Gjelle S (2001). Strontium and carbon isotope geochemistry applied to dating of carbonate sedimentation: an example from high-grade rocks of the Norwegian Caledonides. Precambrian Res 108: 267-292.

Narbonne GM, Kaufman AJ, Knoll AH (1994). Integrated chemostratigraphy and biostratigraphy of the Windermere Supergroup, northwestern Canada: implications for Neoproterozoic correlations and the early evolution of animals. Geol Soc Am Bull 106: 1281-1292.

Onimisi M, Obaje NG, Daniel A (2013). Geochemical and petrogenetic characteristics of the marble deposit in Itobe area, Kogi state, Central Nigeria. Adv Appl Sci Res 4: 44-57.

Pandit MK, Sial AN, Jamrani SS, Ferreira VP (2001). Carbon isotopic profile across the Bilara Group rocks of Trans-Aravalli Marwar Supergroup in western India: implications for Neoproterozoic – Cambrian transition. Gondwana Res 4: 387-394.

Pandit MK, Sharma KK, Sial AN, Ferreira VP (2009). C- and O-isotopic characteristics of Neoproterozoic Sirohi Group meta-carbonates in NW India and their palaeoclimatic implications. Curr Sci 97: 246-251.

Plašienka D (1981). Tectonic position of some metamorphosed Mesozoic sequences of Veporic unit. PhD, Geological Institute of the Slovak Academy of Sciences, Bratislava, Slovakia.

Plašienka D (1983). Geologic structure of the Tuhár Mesozoic. Miner Slovaca 15: 49-58 (in Slovak).

Plašienka D (1993). Structural pattern and partitioning of deformation in the Veporic Foederata cover unit (Central Western Carpathians). In: Rakús M, Vozár J, editors. Geodynamic Evolution and Abyssal Structure of Western Carpathians. Bratislava, Slovakia: State Geological Institute of Dionýz Štúr, pp. 269-277 (in Slovak).

Qadhi TM (2008). Testing Jabal Farasan marble deposit for multiple industrial applications. Arab J Sci Eng 33: 79-97.

Richardson CK, Rye RO, Wasserman MD (1988). The chemical and thermal evolution of the fluids in the Cave-in-Rock fluorspar district, Illinois: stable isotope systematics at the Deardorff Mine. Econ Geol 83: 765-783.

Rollinson HR (1993). Using Geochemical Data: Evaluation, Presentation, Interpretation. London, UK: Longman Singapore Publishers.

Rosenbaum J, Sheppard SMF (1986). An isotopic study of siderites, dolomites and ankerites at high-temperatures. Geochim Cosmochim Acta 50: 1147-1150.

Rozlozsnik P (1935). Die geologischen Verhältnisse der Umgebung von Dobsina. Geol Hung Ser Geol 5: 2-24 (in German).

Ružička P (2009). Metamorphic evolution of a carbonate complex from the Foederata Group (Southern Veporicum, Western Carpathians). PhD, Comenius University in Bratislava, Bratislava, Slovakia.

Ružička P, Vozárová A, Michálek M, Dyda M (2011). Alpine regional metamorphism of Föderata Group metacarbonates (southern Veporicum, Western Carpathians, Slovakia): P–T conditions of recrystallization. Geol Quart 55: 9-26.

Sass E, Katz A (1982). The origin of platform dolomites: new evidence. Am J Sci 282: 1184-1213.

Shearman DJ, Shirmohammadi NH (1969). Distribution of strontium in dedolomites from the French Jura. Nature 223: 606-608.

Stakes DS, O'Neil JR (1982). Mineralogy and stable isotope geochemistry of hydrothermally altered oceanic rocks. Earth Planet Sci Lett 57: 285-304.

Straka P (1981). About the age of Foederata. Geol Práce Spr 75: 57-62 (in Slovak).

Swart PK, Burns SJ, Leder JJ (1991). Fractionation of the stable isotopes of oxygen and carbon in carbon dioxide during the reaction of calcite with phosphoric acid as a function of temperature and technique. Chem Geol 86: 89-96.

Tanaka K, Kawabe I (2006). REE abundances in ancient seawater inferred from marine limestone and experimental REE partition coefficients between calcite and aqueous solution. Geochem J 40: 425-435.

Tanaka M, Shimizu H, Masuda A (1990). Features of the heavy rare-earth elements in seawater. Geochem J 24: 39-46.

Taylor SR, McLennan SM (1981). The composition and evolution of the continental crust: rare earth element evidence from sedimentary rocks. Phil Trans Roy Soc London Ser A 301: 381-399.

Taylor SR, McLennan SM (1985). The Continental Crust: Its Composition and Evolution. 1st ed. London, UK: Blackwell.

Tucker ME (1983). Diagenesis, geochemistry, and origin of a Precambrian dolomite: the Beck Spring Dolomite of eastern California. J Sediment Petrol 53: 1097-1119.

Turekian KK, Wedepohl KH (1961). Distribution of the elements in some major units of the earth's crust. Geol Soc Am Bull 72: 175-192.

Veizer J (1983). Chemical diagenesis of carbonates: theory and application of trace element technique. In: Arthur MA, Anderson TF, Kaplan IR, Veizer J, Land LS, editors. Stable Isotopes in Sedimentary Geology. Short Course Notes 10. Tulsa, OK, USA: SEPM, pp. 3.1-3.100.

Vojtko R, Hók J, Kováč P, Madarás J, Filová I (2000). Geological structure and tectonic evolution of the Southern Veporicum. Slovak Geol Mag 6: 287-292.

Vozár J, Káčer Š, Bezák V, Elečko M, Gross P, Konečný V, Lexa J, Mello J, Polák M, Potfaj M et al., editors (1998). Geological Map of the Slovak Republic 1:1 000 000. Bratislava, Slovakia: State Geological Institute of Dionýz Štúr.

Vozárová A, Vozár J (1982). New lithostratigraphical division of the basal part of the cover of Southern Veporicum. Geol Práce Spr 78: 169-194 (in Slovak).

Vozárová A, Vozár J (1988). Late Paleozoic in West Carpathians. Bratislava, Slovakia: State Geological Institute of Dionýz Štúr.

Vrána S (1966). Alpidische Metamorphose der Granitoide und Foederata-Serie im Mittelteil der Veporiden. Sborník geol vied, rad ZK 6: 29-84 (in German).

Wright IP, Grady MM, Pillinger CT (1988). Carbon, oxygen and nitrogen isotopic compositions of possible Martian weathering products in EETA 79001. Geochim Cosmochim Acta 52: 917-924.